Ecotoxicology and Environmental Safety 302 (2025) 118579

Contents lists available at ScienceDirect

Ecotoxicology and Environmental Safety

journal homepage: www.elsevier.com/locate/ecoenv

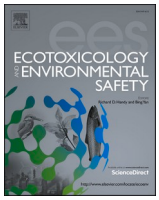

Characterization of known and unknown AhR-active substances in freshwater fish from the Gapcheon River, South Korea: Application of effect-directed analysis and nontarget screening

Jihyun Cha [a], Jiyun Gwak [a], Junghyun Lee [b], Dokyun Kim [c], Eun-Ji Won [d], Kyung-Hoon Shin [d], Hyo-Bang Moon [d], Jong Seong Khim [e], Seongjin Hong [a,*]

[a] Department of Earth, Environmental & Space Sciences, Chungnam National University, Daejeon 34134, Republic of Korea
[b] Department of Environmental Education & Research Institute of Global AI Convergence, Kongju National University, Gonju 32588, Republic of Korea
[c] Marine Environment Research Department, Korea Institute of Ocean Science and Technology, Busan 49111, Republic of Korea
[d] Department of Marine Science and Convergence Engineering, Hanyang University, Ansan 15588, Republic of Korea
[e] School of Earth and Environmental Sciences & Research Institute of Oceanography, Seoul National University, Seoul 08826, Republic of Korea

ARTICLE INFO

Edited by Dr Yong Liang

Keywords:
Bioaccumulation
Persistent toxic substances
Freshwater fish
Aryl hydrocarbon receptor
Effect-directed analysis
Nontarget screening
QSAR modeling

ABSTRACT

This study investigated the distribution and composition of persistent toxic substances in freshwater fish collected from the Gapcheon River, Daejeon, South Korea. To identify key toxicants responsible for biological effects, effect-directed analysis was applied, focusing on aryl hydrocarbon receptor (AhR) agonists. The target species included crucian carp (S1, *Carassius carassius*), common carp (S2, *Cyprinus carpio*), Far Eastern catfish (S3, *Silurus asotus*), barbel steed (S4, *Hemibarbus labeo*), and skygager (S5, *Erythroculter erythropterus*). Trophic positions (TP), estimated from $\delta^{15}N$ values of amino acids, were 2.2 for S1 and S2, 3.0 for S3, and 3.2 for S4 and S5. Concentrations of mercury (Hg), polychlorinated biphenyls, and polycyclic aromatic hydrocarbons (PAHs) exhibited species- and organ-specific patterns, generally increasing with TP. The H4IIE-*luc* bioassay indicated elevated AhR-mediated potencies in mid-polar fractions (F2) from S1 muscle and egg, S3 fillet, and S5 liver. Target analysis of 21 known AhR agonists, including 7 traditional and 14 emerging PAHs, accounted for 20–94 % of total AhR activity, with benzo[*b*]anthracene emerging as the dominant contributor (mean = 44 %). Nontarget screening using GC-QTOFMS on F2 identified 19 AhR agonist candidates, including compounds potentially associated with crude oil and vehicle emissions, combustion byproducts, dye precursors, industrial materials, silicone-based compounds, and natural products. In silico modeling predicted AhR binding potential for all candidates, with triphenylmethane and 1,1,3,3-tetraphenyl-1,3-dimethyldisiloxane showing the highest overall toxic potential. These findings highlight the diversity and ecological relevance of AhR-active contaminants in freshwater fish and their implications for contaminant transfer in aquatic food webs.

1. Introduction

Persistent toxic substances (PTSs) originate from various anthropogenic and industrial activities and are released into the environment (Hu et al., 2023). They are typically characterized by resistance to degradation, bioaccumulation potential, environmental mobility, and toxicity to organisms (Wolska et al., 2012). PTSs encompass a wide range of organic and inorganic pollutants, including mercury (Hg), polychlorinated biphenyls (PCBs), and polycyclic aromatic hydrocarbons (PAHs). Once introduced into the aquatic environments, these contaminants can accumulate in organisms and pose ecological risks through various toxicological mechanisms (Bocio et al., 2007; Kidd et al., 2003; Wang et al., 2012). Hg and PCBs are known to biomagnify through food webs (Bocio et al., 2007; Kidd et al., 2003; Wang et al., 2016), whereas PAHs are typically subject to trophic dilution due to metabolic transformation (An et al., 2020; Qadeer et al., 2019). However, some studies have reported PAHs bioaccumulation under specific environmental conditions (Wang et al., 2012; Zhang et al., 2015). The accumulation patterns of PTSs vary depending on environmental factors, compound-specific properties, and species-specific physiological traits.

Effect-directed analysis (EDA) is a versatile methodology for identifying key toxicants in complex environmental samples such as

* Corresponding author.
E-mail address: hongseongjin@cnu.ac.kr (S. Hong).

https://doi.org/10.1016/j.ecoenv.2025.118579
Received 7 April 2025; Received in revised form 22 June 2025; Accepted 23 June 2025

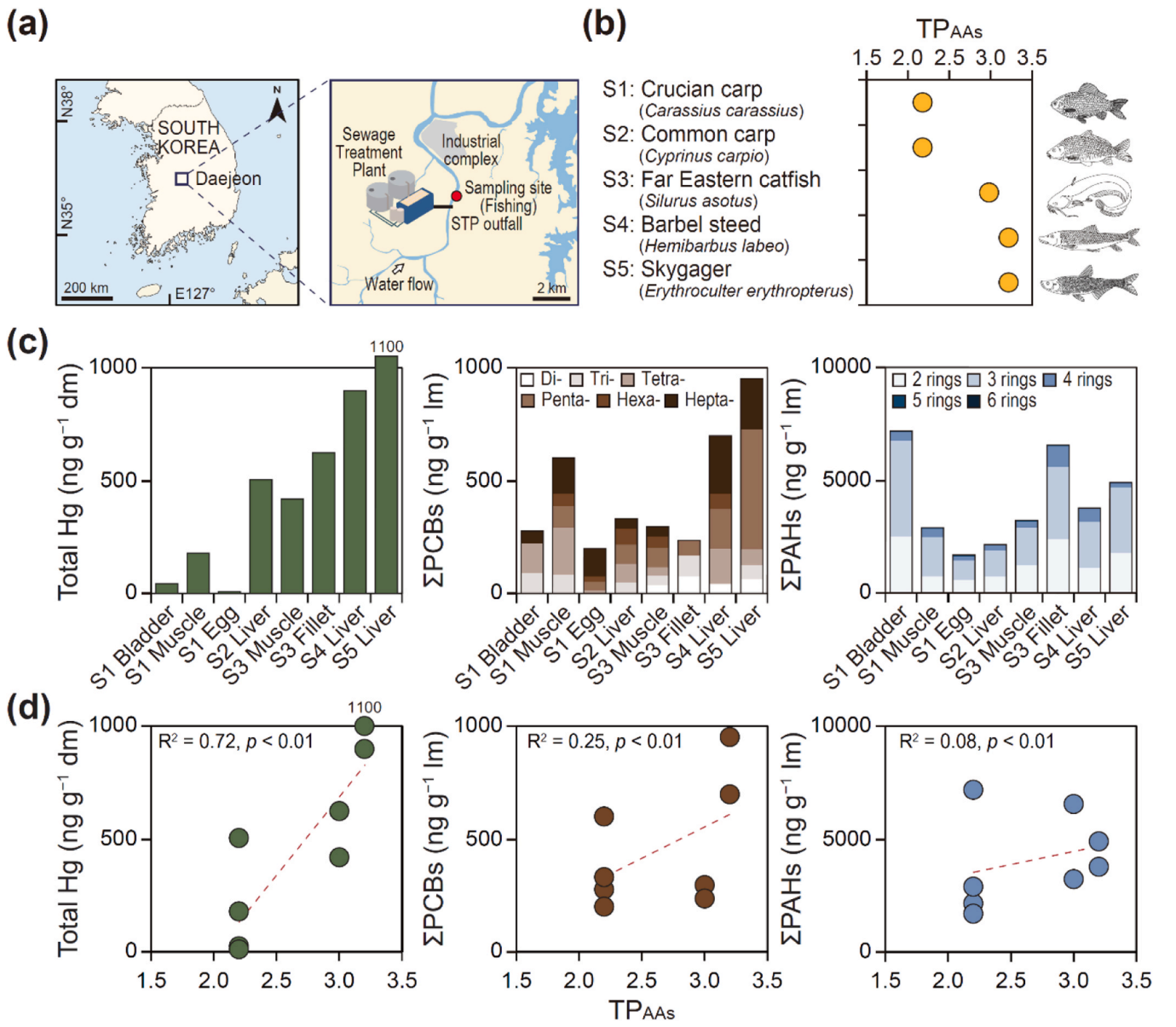

Fig. 1. (a) Map showing the sampling site for freshwater fish from the Gapcheon River, Daejeon, South Korea, including crucian carp (S1, *Carassius carassius*), common carp (S2, *Cyprinus carpio*), Far Eastern catfish (S3, *Silurus asotus*), barbel steed (S4, *Hemibarbus labeo*), and skygager (S5, *Erythroculter erythropterus*). (b) Trophic positions of the collected fish estimated using $\delta^{15}N_{Glu-Phe}$ amino acids. (c) Concentrations of Hg, PCBs, and PAHs in the fish. (d) Relationships between Hg, PCBs, and PAHs and the trophic positions of the fish.

sediments, wastewaters, and biota (Brack, 2003; Hong et al., 2023). By integrating bioassays, fractionation, and instrumental analysis, EDA systematically reduces sample complexity and enables the detection of bioactive fractions (Brack, 2003; Xiang et al., 2024). Effect-based monitoring employs both in vitro and in vivo bioassays to provide a comprehensive evaluation of sample toxicity (Connon et al., 2012; Neale et al., 2023). Fractionation separates substances based on physicochemical properties, and bioassays are subsequently used to assess the toxicity of each fraction (Cha et al., 2022; Simon et al., 2013). Instrumental analysis quantifies target compounds and determines their contribution to the overall toxic effects observed in environmental matrices (Brack et al., 2016).

When known toxic substances cannot fully explain the observed toxicity, nontarget screening (NTS) is applied to identify previously unrecognized compounds (Ruan et al., 2023). Environmental samples typically contain thousands of chemical constituents, making the identification of specific toxicants particularly challenging (Du et al., 2022). Recent advances in high-resolution mass spectrometry (HRMS) have significantly enhanced the detection of unknown substances through comprehensive library-matching techniques (Phillips et al., 2022). HRMS-based NTS allows the comparison of unknown features against extensive chemical databases, facilitating the identification of potential toxicants (Cheng et al., 2024; Zhou et al., 2022). To refine candidate lists, multiple selection criteria, such as peak intensity, spectral match score, and peak shape quality, are applied, systematically narrowing down the most likely contributors (Cha et al., 2022; Hong et al., 2023; Mok et al., 2023).

A major limitation of this approach is the limited availability of reference standards for many chemicals, which constrains the comprehensive identification and toxicity assessment of unknown substances (Cha et al., 2023). To address this challenge, computational modeling for toxicity prediction has gained increasing attention in recent years (Schaupp et al., 2023). In silico models have proven valuable in complementing traditional empirical assessments by enabling toxicity

prediction for uncharacterized compounds (Bak et al., 2019; Schaupp et al., 2023). These models allow for rapid and cost-effective predictions across multiple ecological levels, from cellular to population and community scales, even with limited structural or physicochemical data (Xie et al., 2022). As a result, the use of *in silico* modeling has become increasingly common in identifying the toxic potential of candidate compounds detected in environmental samples (Black et al., 2021).

The aryl hydrocarbon receptor (AhR) is a ligand-activated transcription factor that mediates toxic responses to a wide range of environmental contaminants (Wilson and Safe, 1998). AhR agonists include both hydrophobic and hydrophilic compounds, including PCBs, PAHs, dioxins and furans, pharmaceuticals, and pesticides (Cha et al., 2023; Koh et al., 2004; Lee et al., 2022; Ruan et al., 2023). These chemicals, commonly used in industrial, agricultural, and domestic applications, often enter aquatic environments through surface runoff, atmospheric deposition, and sewage treatment plant (STP) effluents (Escher et al., 2020). Once introduced into aquatic ecosystems, they can accumulate in organisms and be transferred across trophic levels within food webs (Cha et al., 2022, 2023). Recent studies have detected AhR agonists in top marine predators, such as cetaceans and seagulls (Cha et al., 2022, 2023), suggesting the potential for long-range transport and biomagnification of these substances. While much of the research has focused on their presence and effects in high-trophic marine species, comparatively little is known about their impact on lower-trophic-level organisms, particularly freshwater fish. Due to their constant exposure to waterborne contaminants and their central roles in aquatic ecosystems, freshwater fish are especially vulnerable to AhR-active compounds (Lille-Langøy et al., 2021). As such, they serve as critical bioindicators for evaluating ecological risks and the health of freshwater environments.

This study aimed to investigate the distribution and composition of PTSs in freshwater fish collected from the Gapcheon River, Daejeon, South Korea. Targeted PTSs included Hg, PCBs, and PAHs to examine key factors influencing their accumulation patterns and tissue-specific distributions in freshwater fish. To identify the key toxicants responsible for toxicological effects in fish extracts, EDA was conducted with a particular focus on AhR agonists. Compound-specific isotope analysis of amino acids was applied to determine the trophic positions of fish. AhR-active fractions in fish extracts were identified using the H4IIE-*luc* bioassay, and the contribution of targeted AhR agonists to the total bioassay-derived activity was quantified. NTS was applied to detect previously unrecognized AhR-active compounds in toxic fractions, followed by in silico modeling to predict their AhR binding affinity. Additionally, in silico modeling was applied to predict potential toxicological effects of AhR agonist candidates. To our knowledge, this study is the first to apply the EDA approach to identify major AhR agonists across both trophic levels and organ types in freshwater fish from an urban river. It provides new insights into the species- and organ-specific distributions of AhR agonists in freshwater ecosystems and their potential roles in contaminant bioaccumulation and ecological risk.

2. Materials and methods

2.1. Sample collection and preparation

The Gapcheon River, located in Daejeon City, South Korea, is the primary tributary of the Geum River, with a basin area of 648.87 km^2 and a total length of 73.70 km (Jang et al., 2019). As it flows through Daejeon, the river receives effluent from the Daejeon STP (Fig. 1a) (Gwak et al., 2022b). Despite improvements to the combined sewer systems, pollution remains a concern due to discharges from the STP and aging urban infrastructure. In April 2022, freshwater fish, including crucian carp (S1, *Carassius carassius*), common carp (S2, *Cyprinus carpio*), Far Eastern catfish (S3, *Silurus asotus*), barbel steed (S4, *Hemibarbus labeo*), and skygager (S5, *Erythroculter erythropterus*), were collected using hand nets. Biological information on the collected fish is provided in Table S1 of the Supplementary Materials. Immediately after collection, tissues were dissected on-site to determine the organ-specific accumulation of contaminants. Considering the amount of samples, bladder, muscle, and egg of S1, muscle and fillet of S3, and liver of S2, S4, and S5 were selected as test samples for EDA in this study. All samples were transferred to glass vials, stored in ice, and subsequently frozen at –20 °C until analysis.

2.2. Analysis of carbon and nitrogen stable isotopes and trophic position calculation

Stable carbon and nitrogen isotope ratios ($\delta^{13}C$ and $\delta^{15}N$) were analyzed in fish tissues (muscle). Analytical methods followed those described by Lorrain et al. (2003). Bulk carbon and nitrogen isotope ratios were measured using an elemental analyzer (EA, Vario PYROcube, Elementar, Langenselbold, Germany) coupled with an isotope ratio mass spectrometer (Isoprime100, Isoprime LTD., Manchester, UK). Compound-specific nitrogen stable isotope ratios of amino acids ($\delta^{15}N_{AAs}$) were also determined (Chikaraishi et al., 2009; Kim et al., 2022). Approximately 3.0–5.0 mg of freeze-dried samples were hydrolyzed with 12 M hydrochloric acid at 110 °C for 12 h. The hydrolysates were derivatized using thionyl chloride/isopropanol (1:4, v/v) at 110 °C for 2 h, followed by pivaloyl chloride/DCM (1:4, v/v). Derivatized amino acids were extracted with hexane/DCM (3:2, v/v). The $\delta^{15}N$ values of individual amino acids were analyzed using gas chromatography (Agilent GC 6890 N, Agilent Technologies, Santa Clara, CA) coupled with an isotope ratio mass spectrometer (Isoprime, GV Instruments). TPs were calculated using the $\delta^{15}N$ values of glutamic acid ($\delta^{15}N_{Glu}$, trophic amino acid) and phenylalanine ($\delta^{15}N_{Phe}$, source amino acid) according to Eq. 1:

$$TP_{Glu-Phe} = \left(\frac{\delta^{15}N_{Glu-Phe} - \beta}{6.9}\right) + 1 \quad \text{(Eq. 1)}$$

The TPs of each fish were calculated using a trophic discrimination factor of 6.9 (Blanke et al., 2017), and β values were set at 3.4 ‰ (Chikaraishi et al., 2009; Minagawa and Wada, 1984). Trophic levels of the fish species used in this study, along with additional species from the same region, were previously reported in a separate publication, which provides further methodological and contextual details (Kim et al., 2025).

2.3. Extraction and fractionation

For organic extraction, 1.0 g of freeze-dried sample was subjected to Soxhlet extraction for 16 h using 350 mL of dichloromethane (DCM, J.T. Baker, Phillipsburg, NJ). The resulting extracts were concentrated to 1.2 mL, of which 0.2 mL was allocated for lipid content analysis. The remaining 1.0 mL was purified using gel permeation chromatography with Bio-Beads S-X3 columns (Bio-Rad Laboratories, Hercules, CA) to remove lipids and other interfering substances. Lipid removal was performed using 350 mL of a 1:1 (v/v) mixture of hexane and DCM (Honeywell, Charlotte, NC). Following lipid removal, 0.2 mL of the raw organic extract (RE) was solvent-exchanged with dimethyl sulfoxide (DMSO, Sigma-Aldrich, Saint Louis, MO) for bioassay testing. The remaining 0.8 mL of RE was fractionated using silica gel column chromatography, resulting in three fractions: non-polar (F1), mid-polar (F2), and polar (F3). These were eluted sequentially with 30 mL of hexane, 60 mL of hexane and DCM mixture (4:1, v/v), and 50 mL of DCM and acetone mixture (3:2, v/v), respectively. The polarity classification of F1, F2, and F3 was based on relative differences among the three solvent systems, rather than absolute polarity indices. This classification has been consistently used in our previous studies (Cha et al., 2022, 2023; Hong et al., 2016) and is also supported by similar terminology in the literature (Totlandsdal et al., 2014). Each fraction was concentrated to 0.8 mL using rotary evaporation and nitrogen gas. Of this, 0.2 mL was exchanged with DMSO for bioassay testing, while 0.6 mL was reserved

for target analysis and NTS. The final extract concentration corresponded to approximately 1.0 g of tissue per 1.0 mL [~1.0 g biota equivalent (BEq) mL^{-1}].

2.4. Target chemical analysis

Target analytes included Hg, 32 PCBs, 15 traditional PAHs (t-PAHs), and 14 emerging PAHs (e-PAHs). t-PAHs refer to the 16 priority PAHs (excluding naphthalene) designated by the United States Environmental Protection Agency (US EPA) due to their known ecological and human health risks (Neff, 1979). e-PAHs are structurally related compounds that are not included in the US EPA's priority list but are increasingly detected in various environmental matrices. These compounds often originate from similar sources and exhibit comparable environmental behaviors and toxicological properties to those of t-PAHs. In recent years, e-PAHs have been frequently reported in sediments from industrialized coastal regions in Korea (Cha et al., 2019; Gwak et al., 2022a; Kim et al., 2019). PCB standards were obtained from Wellington Laboratories (Guelph, ON, Canada), and PAH standards were obtained from ChemService (West Chester, PA) and Sigma-Aldrich. Detailed information on these compounds is provided in Table S2. Hg concentrations in dried fish samples (0.01–0.10 g) were measured using a direct mercury analyzer (DMA-80, Milestone, Sorisole, Italy), with a detection limit of 0.005 ng Hg. Certified reference material (BCR-277R, estuarine sediment, European Community Bureau of Reference, IRMM, Belgium) was analyzed at the beginning and end of each batch for quality control. PCBs and PAHs were quantified in F1 and F2 fractions of the biota extracts, respectively. Prior to instrumental analysis, 100 ng of 2-fluorobiphenly was added as an internal standard to correct for instrumental variability. Procedural blanks were included in every batch and analyzed under identical conditions to monitor potential contamination. PCBs were analyzed using GC-tandem mass spectrometry (Agilent 7890B GC & 7000 C MS/MS, Agilent Technologies), with an HP-5MS column. PAH concentrations were determined using GC-mass selective detector (MSD, Agilent 7890B & 5977B, Agilent Technologies), with a DB-5MS column. Detailed instrument conditions are provided in Tables S3 and S4. No target compounds were detected in procedural blanks. Surrogate standards were not added during extraction and fractionation to prevent potential interferences with AhR bioassay results. However, matrix spike recovery tests using the same protocol were previously conducted on fish tissues from Ulsan Bay, Korea (An et al., 2020), yielding recovery rates of 80–94 % (mean = 87 %) for seven PCBs and 73–87 % (mean = 81 %) for four PAHs. Given the similarity in sample types and extraction protocols, these recovery rates are considered representative of the current dataset (An et al., 2020). Additional validation using NIST SRM 1944 showed recoveries ranging from 52 % to 117 % (mean = 81 %) for PCBs and 45–104 % (mean = 75 %) for PAHs. Limit of detections (LODs) were calculated as 3.143 times the standard deviation of the lowest calibration standard (n = 7).

2.5. H4IIE-luc in vitro bioassays and potency balance analysis

The H4IIE-*luc* bioassay was conducted following protocols described in previous studies (Cha et al., 2023; Hong et al., 2016). Briefly, H4IIE-*luc* cells were detached from the culture plate using trypsin, and suspended at a concentration of approximately 74,000 cells mL^{-1}. The cells were seeded into 96-well plates and incubated for 24 h at 37 °C in a humidified atmosphere with 5 % CO_2. After incubation, the medium was removed, and the positive control (benzo[*a*]pyrene, BaP), solvent control (0.1 % DMSO), negative control (culture medium), and fish extracts were added in triplicate. All samples were adjusted to a final DMSO concentration of 0.1 %. BaP was used as the positive control at a maximum concentration of 50 nM. Serial dilutions of BaP (1:3) were prepared to generate six concentrations (50, 17, 5.6, 1.9, 0.6, and 0.2 nM). Luminescence was measured using a Victor multilabel plate reader and recorded as relative luminescence units (RLUs). To account for DMSO-related background, RLU values for BaP and samples were corrected by subtracting the solvent control (0.1 % DMSO) RLUs. Final results were expressed as percentages relative to the maximum RLU observed for the BaP control. No AhR-mediated activity was detected in the negative control or procedural blanks, confirming the absence of background contamination from sample preparation or experimental procedures. Significant AhR-mediated potencies were calculated by dividing the standard deviation of the RLU values from the solvent control group by the RLU values at the highest concentrations of the positive control, which was 3.3 %BaP.

The AhR agonists among the targeted chemicals and their relative potency (ReP) values are summarized in Table S5. To assess the contribution of each AhR agonist to the overall AhR-mediated activity observed in fish extracts, instrument-derived BaP equivalents (BaP-EQ_{chem}) and bioassay-derived BaP equivalents (BaP-EQ_{bio}) were compared. BaP-EQ_{bio} values were calculated from dose-response curves for samples exhibiting more than 20 % of BaP_{max}. BaP-EQ_{chem} was calculated by multiplying the measured concentrations of each substance by its corresponding ReP.

2.6. Nontarget screening and data processing

NTS was conducted on the most potent fractions using a GC-quadrupole time-of-flight mass spectrometry (GC-QTOFMS, Agilent 7890B GC with a 7200 QTOFMS; Agilent Technologies). Detailed instrumental conditions are provided in Table S6. Data processing was performed using Agilent Unknown Analysis software. Nontarget features were extracted from the raw data via deconvolution (Mok et al., 2023). Retention time (RT) widow factors were set to 50, 100, 200, and 300, with a required number of ion peaks ranging from 3 to 10. The identification of AhR agonist candidates followed a six-step selection process: 1) deconvolution for nontarget feature extraction (Mok et al., 2023), 2) spectral matching with the National Institute of Standards and Technology (NIST) 17 library (Mok et al., 2023), 3) retention time index (RI) filtering using n-alkane standards (Mok et al., 2024), 4) selection of compounds with a matching score $\geq$ 70 (Muz et al., 2017), 5) filtering for aromatic structure (Mekenyan et al., 1996), and 6) narrowing the selection to compounds containing three or more aromatic rings (Gwak et al., 2022a).

2.7. Prediction of additional toxicities of AhR agonist candidates

In silico modeling was conducted using the VirtualToxLab platform to predict the binding affinities of AhR agonist candidates to various cellular receptors, including AhR, androgen receptor (AR), estrogen receptor (ER), glucocorticoid receptor (GR), and thyroxine receptor (TR), considering thermodynamic properties (Vedani et al., 2015). This approach enabled the estimation of toxic potential based on receptor-binding affinity. Additionally, toxicity predictions were conducted using the VEGA quantitative structure-activity relationships (QSARs). VEGA utilizes the SMILES notation of each compound and integrates outputs from multiple models to classify chemicals as active or inactive with respect to various toxicological endpoints (Marzo et al., 2016). VEGA QSARs provided predictions for carcinogenicity, developmental toxicity, and mutagenicity.

2.8. Statistical analysis

Principal component analysis (PCA) was performed using IBM SPSS Statistics 26 (SPSS Inc., Chicago, IL) to evaluate distribution patterns of target substances in freshwater fish. The suitability of the dataset for PCA was confirmed using Bartlett's test and the Kaiser-Meyer-Olkin (KMO) measure, with a KMO value exceeding the recommended threshold of 0.50. The PCA included concentrations of Hg, PCBs, and PAHs. PCBs were grouped by chlorine content, and PAHs were categorized based on the number of aromatic rings. For statistical processing,

concentrations below the LOD were replaced with LOD/2.

3. Results and discussion

3.1. Trophic positions of freshwater fish

The $\delta^{13}C_{bulk}$ values for all fish samples ranged from –23.9 ‰ to –23.1 ‰, indicating a common basal food source (Table S1). In contrast, $\delta^{15}N_{bulk}$ values exhibited substantial variation (9.1 ‰ to 13.8 ‰), reflecting differences in trophic positioning among species. TPs estimated from bulk $\delta^{15}N$ values (TP_{bulk}) ranged from 2.5 to 3.9, while those derived from $\delta^{15}N$ values of amino acids (TP_{AAs}) ranged from 2.2 to 3.2. TP_{bulk} values of fish were consistently higher than TP_{AA}, a trend consistent with previous studies, where bulk $\delta^{15}N$ reflects long-term dietary assimilation, while $\delta^{15}N$ values of specific amino acids (e.g., Glu and Phe) provide more precise trophic estimates (An et al., 2020; Won et al., 2020). Crucian carp (S1) and common carp (S2) exhibited TP_{AA} values of 2.2, confirming their positions at lower trophic levels (Fig. 1b). Crucian carp are widespread in Korean freshwater systems and feed on crustaceans, small fish, insects, and plant material (Moon et al., 2006; Park et al., 2022). Common carp are omnivorous and inhabit diverse freshwater environments, including rivers and lakes (Koehn, 2004). However, the crucian carp and common carp collected from the Gapcheon River in this study had a TP of 2.2, indicating that they were highly dependent on plant materials. Far Eastern catfish (S3) had a TP_{AA} value of 3.0, consistent with its role as a mid-level predator consuming small fish, insect larvae, and crustaceans (Kim et al., 2012). Barbel steed (S4) and skygager (S5) exhibited the highest TP_{AA} values (3.2), positioning them at the top of the trophic hierarchy. Barbel steed primarily feeds on periphytic algae, aquatic insects, tubifex worms, and small crustaceans (Park et al., 2022), while skygager, a known piscivore, preys on crustaceans, aquatic insects, and small fish near the water surface (Kim et al., 2012). These results indicate that the Gapcheon River supports a balanced trophic structure, with freshwater fish occupying a wide range of trophic levels from primary consumers to top predators.

3.2. Concentrations and compositions of PTSs in fish

The concentrations and composition of Hg, PCBs, t-PAHs, and e-PAHs in fish samples were analyzed (Table S7). Hg was detected in all tissue extracts, with concentrations ranging from 17 to 1100 ng g^{-1} dry mass (dm) (Fig. 1c). The highest Hg concentration was found in the S5 liver (1100 ng g^{-1} dm), followed by S4 liver (900 ng g^{-1} dm) and S3 fillet (620 ng g^{-1} dm). Elevated Hg concentrations were generally observed in S3, S4, and S5, corresponding to TP of 3.0 or higher (Fig. 1d). In addition, liver and muscle tissues exhibited higher Hg concentrations, likely due to the strong protein-binding affinity of Hg (Bittarello et al., 2020). A comparison among the S1 bladder (36 ng g^{-1} dm), muscle (180 ng g^{-1} dm), and egg (17 ng g^{-1} dm) suggests the potential maternal transfer of Hg, which is consistent with its limited metabolic elimination in adult fish.

The total concentrations of 32 PCBs ranged from 200 to 950 ng g^{-1} lipid mass (lm), with the highest levels observed in the S5 liver (950 ng g^{-1} lm) and S4 liver (700 ng g^{-1} lm) (Fig. 1c). Similar to Hg, elevated PCB concentrations were associated with higher TPs (Fig. 1d), reflecting their well-documented biomagnification potential in aquatic food webs (An et al., 2020; Driscoll et al., 2013). Notably, the liver consistently showed the highest PCB levels, likely due to its physiological role in detoxification and the accumulation of lipophilic contaminants (Wassur, 2012). PCBs composition was dominated by penta-CBs (mean = 25 %), consistent with patterns reported in fish from Ulsan Bay (Fig. 1c) (An et al., 2020). Moreover, lower-chlorinated congeners were more abundant in species at higher trophic levels, supporting previous findings that such congeners tend to biomagnify in food webs (Bocio et al., 2007; Wang et al., 2016). Interestingly, S1 eggs exhibited higher concentrations of hepta-CBs than the corresponding bladder and muscle tissues, indicating maternal transfer of highly chlorinated PCBs due to their high lipophilicity and metabolic persistence (Jordan-Ward et al., 2022). Differences in PCB congener profiles between the S3 muscle and fillet may reflect organ-specific properties, including variations in protein-lipid interactions that influence PCBs distribution (Listrat et al., 2016; Yordy et al., 2010).

The concentrations of 15 t-PAHs and 14 e-PAHs in freshwater fish ranged from 1500 to 6900 ng g^{-1} lm (mean = 3700 ng g^{-1} lm) and 160 to 560 ng g^{-1} lm (mean = 320 ng g^{-1} lm), respectively (Fig. 1c). The e-PAHs, increasingly recognized as contaminants of concern, have been previously detected in sediments and top marine predators in Korean waters (Cha et al., 2019; Cha et al.; Gwak et al., 2022a; Kim et al., 2019). The highest PAH concentrations were observed in the S1 bladder, which may be attributed to organ-specific accumulation patterns influenced by physiological function or residual retention from early developmental exposure (Price and Mager, 2020). Aside from the S1 bladder, elevated PAH concentrations were observed in S3, S4, and S5, which species corresponding to TPs $\geq$ 3.0 (Fig. 1d). This suggests the biomagnification potential of specific PAHs, particularly those with high lipophilicity and resistance to metabolic breakdown (Qin et al., 2020). Variability in PAH levels among tissues likely reflects differential retention capacities and physiological roles across organs.

Consistent with previous findings, PAHs composition in freshwater fish was dominated by low molecular weight (LMW) compounds, particularly those with two to three aromatic rings (Fig. 1c) (Ololade et al., 2024; Qin et al., 2020). Among these, phenanthrene was the most prevalent, accounting for 40–53 % (mean = 47 %) of total PAHs across all samples. Phenanthrene is a ubiquitous PAH in aquatic environments, frequently detected at elevated levels in fish from major rivers worldwide due to its high lipophilicity and environmental persistence (Ololade et al., 2024; Sun et al., 2006). Although phenanthrene is subject to metabolic degradation and excretion in fish, it has also been shown to induce oxidative stress via redox cycling, contributing to cellular toxicity (Sun et al., 2006). Overall, the concentrations of PTSs exhibited species- and organ-specific patterns, generally increasing with TPs. This suggests that aquatic organisms in the Gapcheon River ecosystems may be subjected to chronic exposure and potential biological stress caused by PTSs.

3.3. Bioaccumulation characteristics of PTSs in fish

The bioaccumulation patterns of PCBs and PAHs in fish were further examined in relation to their octanol-water partition coefficients (log K_{OW}) (Fig. S1). PCB concentrations remained relatively consistent across log K_{OW} values, suggesting a broad retention capability within fish tissues regardless of hydrophobicity. In contrast, PAHs with log K_{OW} values exceeding 5.0 exhibited a marked decrease in concentration. This divergence likely reflects differences in metabolic resistance and elimination efficiency between the two compound classes (Snyder et al., 2015). Specifically, high molecular weight (HMW)-PAHs, characterized by greater log K_{OW} values, are more readily metabolized and excreted than LMW-PAHs, resulting in preferential accumulation of LMW-PAHs in fish tissues (Baumard et al., 1998; Wang et al., 2016). Moreover, PAHs with log K_{OW} values below 5.0 may be more efficiently taken up via gill-water exchange, contributing to their elevated levels in aquatic organisms (Cheung et al., 2007). To further elucidate the distribution patterns of PTSs, PCA was performed based on the concentrations of Hg, PCBs, and PAHs in fish tissue extracts (Fig. S1). PC1 and PC2 accounted for 64.3 % and 15.8 % of the total variance, respectively. The PCA results revealed two distinct clusters. The first cluster, comprising primarily samples from higher trophic-level species, showed strong associations with Hg and 2-, 3-, and 4-ring PAHs, along with moderate correlations with di-, tri-, and penta-chlorinated PCBs and 5-ring PAHs. The second cluster, associated with fish from lower trophic levels, exhibited weaker correlations with HMW compounds, such as tetra-, hexa-, and hepta-chlorinated PCBs and 6-ring PAHs. These findings

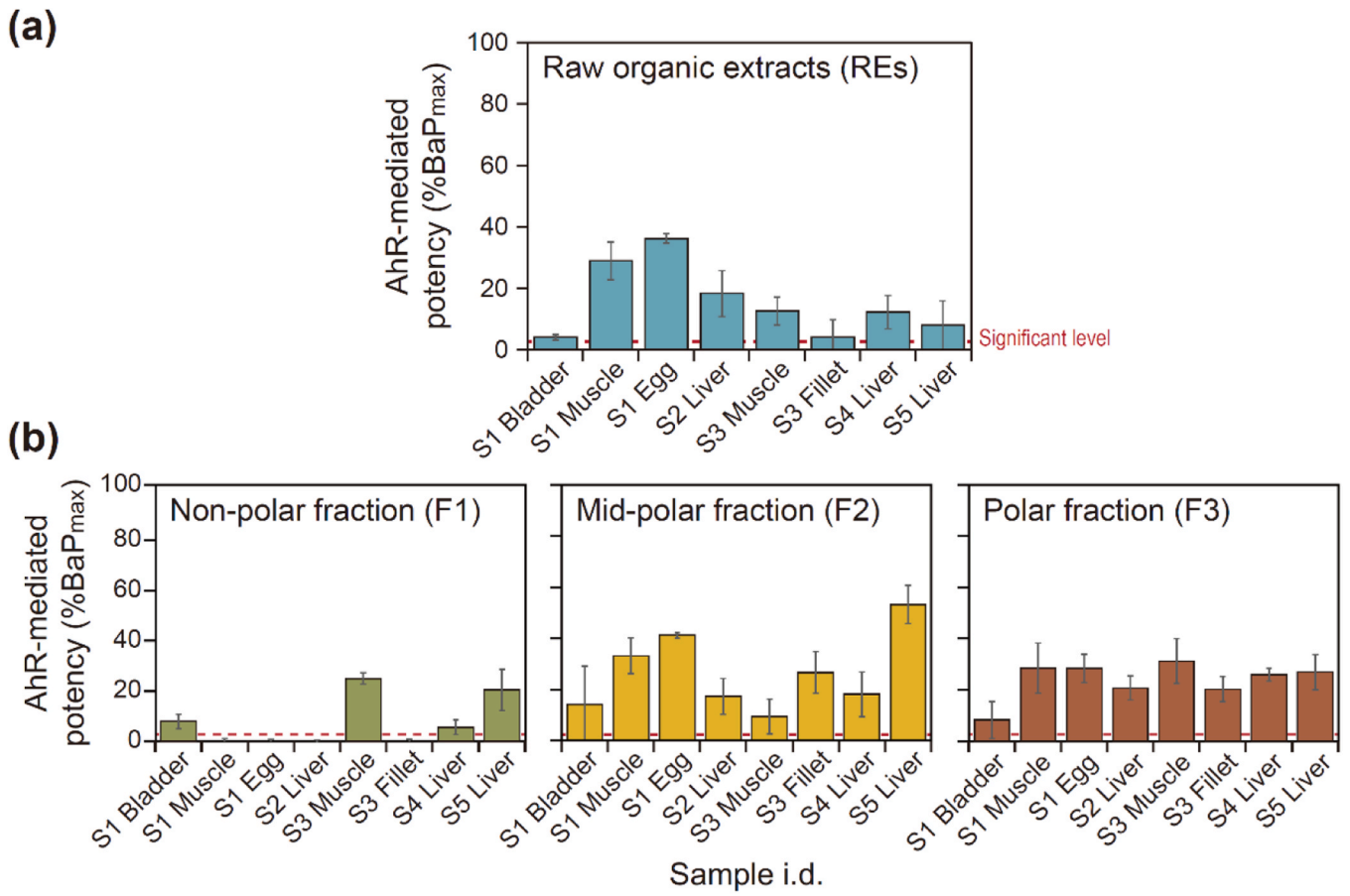

Fig. 2. (a) AhR-mediated potencies in raw organic extracts (REs) from fish samples. (b) AhR-mediated potencies in silica gel fractions, including non-polar (F1), mid-polar (F2), and polar (F3) fractions. The red dotted line indicates the significance threshold for AhR-mediated potencies (3.3 %BaP_{max}). Error bars represent the mean ± standard deviation (n = 3).

Table 1
Potency balance between concentrations of BaP-EQ_{chem} and BaP-EQ_{bio} in mid-polar fractions of fish extracts collected from Gapcheon River, South Korea.

Compounds	Abb.[a]	S1 Muscle	S1 Egg	S3 Fillet	S5 Liver
t-PAHs					
Benzo[*a*]anthracene	BaA	ND[b]	ND	1.1	ND
Chrysene	Chr	2.9	2.5	3.5	1.5
Benzo[*b*]fluoranthene	BbF	ND	ND	ND	ND
Benzo[*k*]fluoranthene	BkF	1.5	2.1	0.65	ND
Benzo[*a*]pyrene	BaP	1.2	0.67	1.4	1.0
Indeno[*1,2,3-cd*]pyrene	IcdP	ND	ND	ND	ND
Dibenz[*a,h*]anthracene	DbahA	ND	ND	ND	2.0×10^{-1}
e-PAHs					
11H-Benzo[*a*]fluorene	11BaF	7.0×10^{-1}	ND	ND	ND
4,5-Methanochrysene	4,5MC	3.8×10^{-1}	3.6×10^{-1}	5.1×10^{-1}	3.7×10^{-1}
Benzo[*b*]anthracene	BbA	10	52	51	57
10-Methylbenzo[*a*]pyrene	10MbA	ND	1.3×10^{-1}	ND	1.7×10^{-1}
20-Methylcholanthrene	20Mc	0.62	0.72	1.0	1.5
7-Methylbenz[*a*]anthracene	7MbA	ND	ND	ND	ND
7,12-Dimethylbenz[*a*]anthracene	7,12DbA	ND	1.0×10^{-1}	ND	ND
11H-Benzo[*b*]fluorene	11BbF	8.0×10^{-2}	ND	2.5×10^{-1}	8.0×10^{-2}
Benzo[*b*]naphtho[*2,1-d*]thiophene	BBNT	ND	ND	2.0×10^{-2}	ND
Benzo[*b*]naphtho[*2,3-d*]furan	BBNF	7.5×10^{-1}	5.6×10^{-1}	2.6×10^{-1}	3.1×10^{-1}
Benzo[*j*]fluoranthene	BjF	ND	ND	ND	ND
5-Methylbenzo[*a*]anthracene	5MbA	ND	ND	ND	ND
1-Methylchrysene	1MC	ND	ND	ND	ND
3-Methylchrysene	3MC	1.8	2.3	3.1	1.7
BaP-EQ_{chem} (ng g^{-1} dm)[c]		20	61	63	64
BaP-EQ_{bio} (ng g^{-1} dm)		21	120	76	320
Contribution (%)		94	49	83	20

[a] Abbreviations.
[b] ND: Not detected.
[c] Calculated by multiplying the concentrations of AhR agonists by their ReP values.

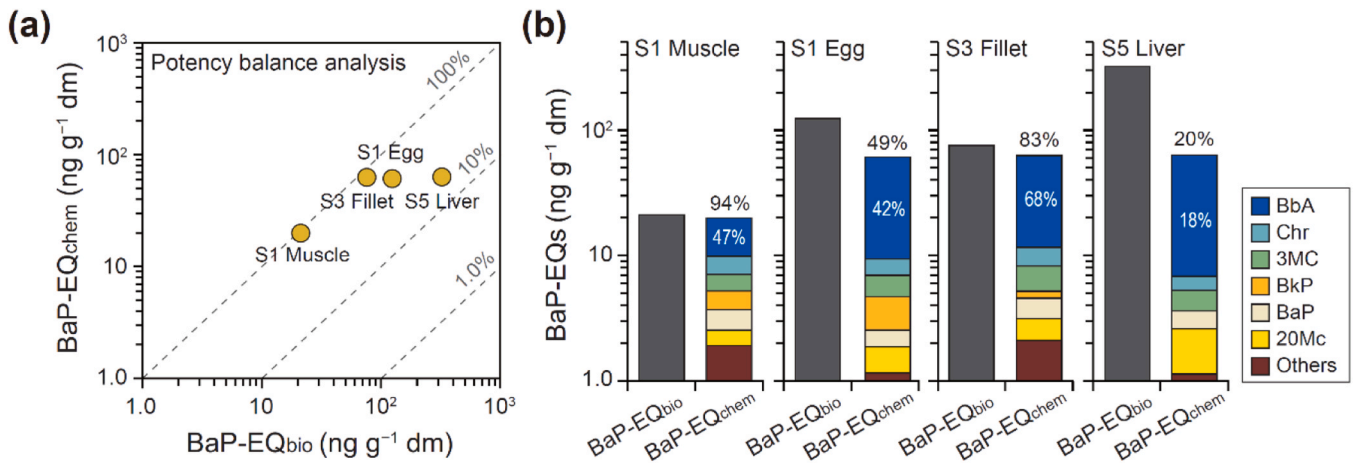

Fig. 3. (a) Potency balance analysis comparing bioassay-derived BaP-EQ$_{bio}$ and instrument-derived BaP-EQ$_{chem}$ in F2 fractions from S1 muscle, S1 egg, S3 fillet, and S5 liver. (b) Contribution of major AhR agonists to the total AhR-mediated potency in each sample.

suggest that trophic level, organ characteristics, and log K_{OW} are key factors controlling the accumulation and distribution of PTSs in freshwater fish.

3.4. AhR-mediated potencies in fish

All REs of fish exhibited significant AhR-mediated potencies in the H4IIE-*luc* bioassay, irrespective of tissue type or TP (Fig. 2a). These results indicate the presence of AhR agonists in fish tissues from Gapcheon River and highlight potential toxicological risks for resident organisms. Analysis of the silica gel fractions revealed that F1 showed markedly higher AhR-mediated potencies in S3, S4, and S5, species characterized by TP (Fig. 2b). This pattern observed in F1 suggests enhanced accumulation of lipophilic AhR agonists in higher TP fish. Consistent AhR activities were also detected in F2 and F3 across all samples, with F2 exhibiting a slightly higher mean potency (27 %) compared to F3 (24 %). The AhR-mediated potencies observed in F2 and F3, unlike those in F1, suggest that the distribution of AhR agonists in mid-polar and polar fractions may be influenced by factors beyond trophic position, including compound polarity, metabolic transformation, and tissue-specific properties. In particular, mid-polar and polar compounds, which are more readily bioavailable, may accumulate in fish, undergo metabolic transformation, and exhibit tissue-specific distribution. These combined factors may contribute to the observed AhR activity. Thus, such confounding variables should be considered collectively when interpreting species-wide patterns of AhR-mediated responses. Notably, BaP_{max} values exceeding 20 % were observed in F2 and F3 of the S1 muscle, S1 egg, S3 fillet, and S5 liver, indicating the presence of potent AhR agonists in mid-polar and polar fractions. These species- and organ-specific AhR responses likely reflect differences in contaminant accumulation and metabolic capacity (Doering et al., 2012).

In this study, additional analyses were conducted focusing on F2, which exhibited relatively high AhR-mediated potencies. Compounds eluted in F2 generally possess lower polarity than those in F3 and tend to have higher log K_{OW} values, indicating a greater potential for bioaccumulation (Kelly et al., 2007). For samples in which F2 exhibited BaP_{max} values above 20 %, BaP-EQ$_{bio}$ concentrations were calculated using the EC_{20}-derived dose-response curve (Fig. S2). The resulting BaP-EQ$_{bio}$ values were 21, 120, 76, and 320 ng BaP-EQ g^{-1} dm for S1 muscle, S1 egg, S3 fillet, and S5 liver, respectively (Fig. S2 and Table 1). Among these, the S5 liver, associated with the highest TP, showed the greatest BaP-EQ$_{bio}$ concentration. Interestingly, the BaP-EQ$_{bio}$ concentration for the S1 egg exceeded that of the S1 muscle, which may be attributed to the high lipid content in eggs, promoting the accumulation of lipophilic contaminants (Hansen et al., 2022; Lee et al., 2017). In addition, the comparatively low metabolic activity in eggs may contribute to prolonged retention of such compounds, further enhancing AhR-mediated potency (Bik et al., 2020). Notably, the substantial AhR activities observed in F3 emphasize the potential role of polar compounds in receptor activation. Given the proximity of sampling sites to the STP outfall, the detection of polar AhR agonists in F3 suggests potential inputs from wastewater effluents (Cha et al., 2021). Previous studies have reported that polar AhR agonists, including pharmaceuticals, pesticides, and steroid hormones, can be detected in aquatic biota and sediments, particularly in industrial and urban environments (Cha et al., 2021, 2022, 2023). More recently, phenolic compounds from household and personal care products have also been shown to contribute to AhR activity (Weiss et al., 2024). These findings suggest that polar substances may contribute to the observed activity in the F3 fraction. Moreover, it is plausible that the biotransformation of non-polar and mid-polar contaminants into more polar metabolites contributes to the observed AhR-mediated responses in freshwater fish (Zhang et al., 2022). However, identifying these polar compounds remains challenging due to the lack of standardized protocols for extraction, purification, and instrumental analysis in biological matrices (Cambiaghi et al., 2017).

3.5. Contribution of known AhR agonists to total AhR-mediated potencies

Potency balance analysis was conducted on F2 from the S1 muscle, S1 egg, S3 fillet, and S5 liver, samples in which AhR-mediated potencies exceeded 20 % of BaP_{max} in the H4IIE-*luc* bioassay. Among the targeted compounds, PCBs and PAHs are well-documented AhR agonists (Lee et al., 2022; Ruan et al., 2023). While PCBs typically require prolonged exposure to elicit a full AhR response in the H4IIE-*luc* assay (Lee et al., 2013; Suzuki et al., 2006), PAHs are known to induce rapid AhR activation, achieving maximum binding within approximately 4 h (Masunaga et al., 2004). During silica gel fractionation, non-polar PCBs predominantly elute in F1, whereas mid-polar PAHs are recovered in F2. The greater AhR-mediated potencies observed in F2 compared to F1 suggest that PAHs are the primary contributors to AhR activity detected in these samples.

The total concentrations of identified AhR agonists were 19, 21, 21, and 13 ng g^{-1} dm in the S1 muscle, S1 egg, S3 fillet, and S5 liver, respectively. Despite the S5 liver exhibiting the highest total PAH concentration among the four samples, it showed the lowest concentration of quantified AhR agonists. This discrepancy may be partially attributed to differences in lipid content across organs; however, it also suggests that PAHs with high log K_{OW} values (> 5.0), although prone to hepatic accumulation, may be subject to rapid biotransformation and

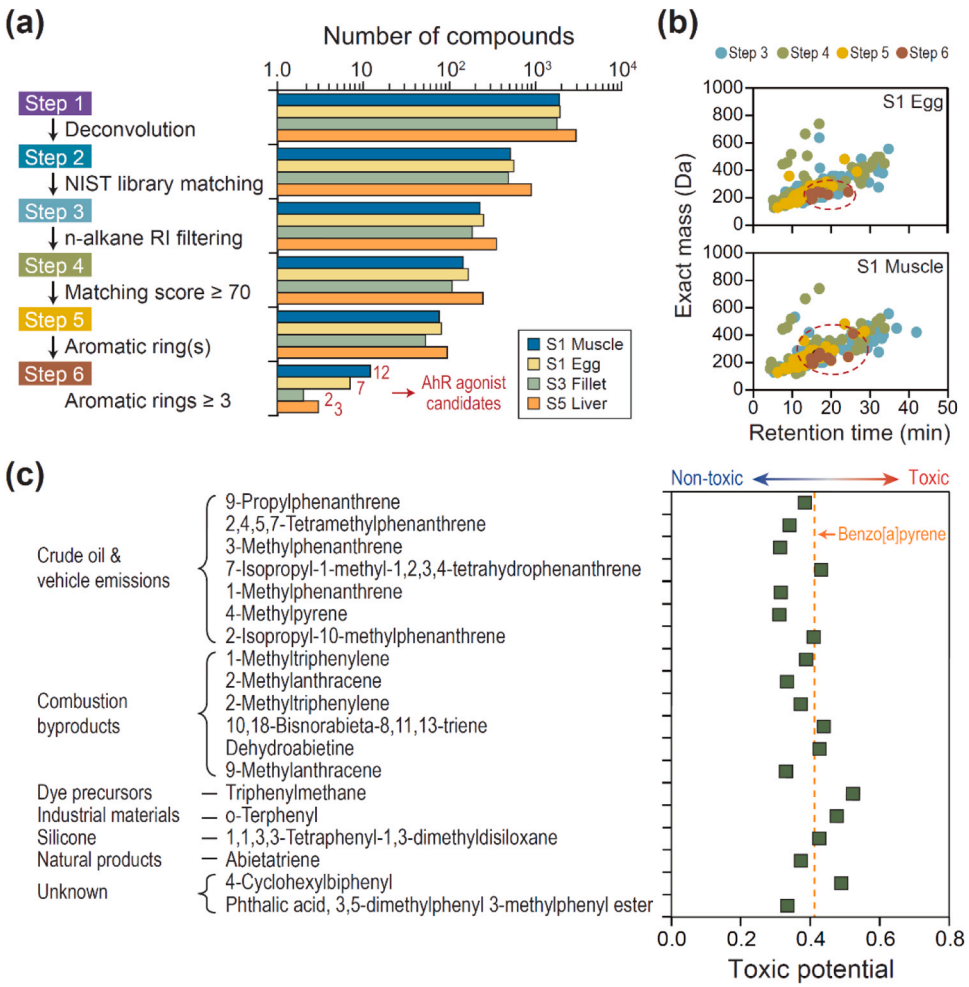

Fig. 4. (a) Data analysis workflow for nontarget screening using GC-QTOFMS, including a six-step selection process to identify AhR agonists in F2 from S1 muscle, S1 egg, S3 fillet, and S5 liver extracts. (b) Retention time and exact mass distribution of AhR agonist candidates refined through the selection process (e.g., S1 muscle and S1 egg samples). Results for S3 fillet and S5 liver samples are shown in Fig. S3. (c) Potential sources of the 19 identified AhR agonist candidates and their predicted AhR binding affinities, assessed using VirtualToxLab in silico modeling. Binding affinity interpretations are as follows: 0.0–0.2 (no binding), 0.2–0.4 (low binding), 0.4–0.6 (moderate binding), and 0.6–0.8 (high binding).

elimination in the liver due to its high metabolic capacity (Wassur, 2012). Among the seven targeted AhR-active t-PAHs, five were detected in at least one fish extract. Chrysene was detected in all samples and exhibited the highest mean concentration (0.55 ng g^{-1} dm). Of the 14 AhR-active e-PAHs, 10 compounds were detected, with benzo[*b*]naphtho[*2,1-d*]furan (BBNF) consistently found in all samples at the highest concentration (mean = 0.99 ng g^{-1} dm). BBNF, a combustion-derived compound primarily emitted from municipal solid waste incineration, has been frequently reported in sediments from industrial regions (Kim et al., 2019; Li and Ellis, 2015). Among the AhR agonists, several e-PAHs, including benzo[*b*]anthracene (BbA), 3-methylchrysene (3MC), 20-methylcholanthrene, 4,5-methanochrysene, and 10-methylbenzo[*a*]pyrene, exhibited RePs exceeding that of BaP, indicating their substantial contribution to overall AhR-mediated effects.

The 15 targeted AhR agonists accounted for 94 %, 49 %, 83 %, and 20 % of the total AhR-mediated potencies in F2 from S1 muscle, S1 egg, S3 fillet, and S5 liver, respectively (Fig. 3a and Table 1). The contributions of t-PAHs and e-PAHs to the observed bioassay responses ranged from 0.86 % to 26 % (mean = 10 %) and from 19 % to 74 % (mean = 52 %), respectively, indicating that e-PAHs were the predominant contributors to overall AhR-mediated activity. Among these compounds, BbA emerged as the most prominent contributor, accounting for 18–68 % (mean = 44 %) of the total potency (Fig. 3b). Notably, BbA has also been identified as a major contributor to AhR-mediated activity in industrial sediments from coastal areas such as Lake Sihwa and Yeongil Bay in Korea (Cha et al., 2019; Gwak et al., 2022a). Consistent with these findings, the present study demonstrates that BbA may also play a significant role in AhR-mediated potencies in freshwater ecosystems. BbA, a compound widely used in the manufacturing of transistor films, possesses a rigid planar molecular structure that confers high metabolic resistance, thereby enhancing its ReP in AhR activation assays (Flesher and Lehner, 2016). Moreover, the linear molecular configuration of BbA reduces its aqueous solubility compared to more angular PAH analogues (Nagpal, 1993), promoting its sorption to biological tissues. Freshwater fish are particularly susceptible to such accumulation due to their constant exposure to waterborne contaminants via gill respiration, which facilitates efficient uptake and retention of hydrophobic compounds (Kelly et al., 2007). Notably, BbA maintained considerable AhR-mediated efficacy throughout the 72-h exposure period in the H4IIE-*luc* bioassay, suggesting limited metabolic degradation under the assay conditions (Lee et al., 2022). Additionally, the relatively lower log K_{OW} of BbA compared to other high ReP compounds may also contribute to its enhanced accumulation and slower metabolism in freshwater, further amplifying its AhR-mediated effects.

Chrysene and 3MC consistently contributed substantially in all samples except for the S5 liver. These findings suggest that the freshwater fish in the Gapcheon River, which shares similar habitats and dietary sources, are likely exposed to common AhR-active contaminants.

While the targeted AhR agonists explained a large proportion of the observed AhR activity in F2 from the S1 muscle and S3 fillet, they accounted for only a partial fraction of the bioassay response in the S1 egg and S5 liver. In the case of the S1 egg, maternal transfer may introduce unmonitored substances that undergo in vivo metabolic transformation, potentially generating novel metabolites with AhR agonistic activity (Russell et al., 1999). Furthermore, the liver, as the principal organ for xenobiotic accumulation, metabolism, and redistribution (van der Oost et al., 2003), may harbor additional AhR-active compounds not targeted in this study. These unidentified substances, including potential metabolites or transformation products, could contribute to the observed residual bioassay responses, highlighting the limitations of chemical-targeted approaches in fully accounting for AhR-mediated effects. For example, retene, a PAH-like compound originating from sources such as the incomplete combustion of carbonaceous materials and effluents from pulp and paper mills, can bioaccumulate in fish and be metabolized into transformation products that have been shown to contribute to AhR activity (Koistinen et al., 1998; Oikari et al., 2002; Ramdahl, 1983; Rude et al., 2024).

3.6. Identification of novel AhR agonists

NTS using GC-QTOFMS was conducted to identify potential AhR agonists in F2 of the S1 muscle, S1 egg, S3 fillet, and S5 liver (Fig. 4a and Table S8). A six-step selection process was employed to refine thousands of initial nontarget features. This process included spectral deconvolution (Mok et al., 2023), NIST library matching (Cha et al., 2019; Kim et al., 2019), RI filtering (Mok et al., 2024), and reliability scoring (Muz et al., 2017). In the final steps, candidates were further screened based on molecular characteristics associated with AhR binding potential, such as aromaticity (Mekenyan et al., 1996) and structure complexity, particularly the presence of three or more aromatic rings (Gwak et al., 2022a). This systematic approach ultimately identified 12, 7, 2, and 3 AhR agonist candidates in the S1 muscle, S1 egg, S3 fillet, and S5 liver, respectively. Among the identified 24 AhR agonist candidates, triphenylmethane was detected in all samples (Table S9). Additionally, 2-isopropyl-10-methylphenanthrene was commonly found in the S1 muscle and S5 liver, while *o*-terphenyl was detected in the S1 muscle and egg. Notably, only one AhR agonist candidate overlapped between the muscle and egg of the same species (S1), indicating distinct compound distribution profiles across different tissues.

The 19 identified AhR agonist candidates exhibited RTs ranging from 14 to 26 min and molecular weights between 192 and 410 Da (Fig. 4b and Fig. S3 and S4). These RT and molecular weight ranges were generally consistent with those observed for known AhR agonists (Cha et al., 2019; Gwak et al., 2022a; Kim et al., 2019). The compounds originated from both anthropogenic and natural sources, including crude oil, vehicle emissions, combustion byproducts, dye precursors, industrial materials, silicone-related compounds, natural products, and unknown sources (Fig. 4c). This suggests that freshwater fish inhabiting urban sites affected by STP effluents are likely exposed to anthropogenic contaminants from these sources, either directly or via environmental transport. Among them, seven compounds were associated with crude oil and vehicle emission, including six alkylated phenanthrene derivates (9-propylphenanthrene, 2,4,5,7-tetramethylphenanthrene, 3-methylphenanthrene, 7-isopropyl-1-methyl-1,2,3,4-tetrahydrophenanthrene, 1-methylphenanthrene, and 2-isopropyl-10-methylphenanthrene), as well as 4-methylpyrene (Huang et al., 2017; Ndabambi et al., 2021; Ogbesejana et al., 2019). These substances may enter urban rivers through vehicle exhaust, industrial emissions, or incomplete removal by STP. Although phenanthrene itself lacks AhR binding affinity in H4IIE-*luc* bioassays, its alkylated derivatives exhibit increased AhR affinity and transcriptional activation due to structural modifications (Lille-Langøy et al., 2021). Notably, both 3-methylphenanthrene and 1-methylphenanthrene have been reported as AhR-binding compounds using a yeast reporter assay system (Sun et al., 2014). Alkylated PAHs are also known to be more toxic than their parent compounds, particularly during early developmental stages in fish, due to biotransformation processes (Lille-Langøy et al., 2021).

Several other compounds (1-methyltriphenylene, 2-methylanthracene, 2-methyltriphenylene, 10,18-bisnorabieta-8,11,13-triene, dehydroabietine, and 9-methylanthracene) were identified as combustion byproducts (An et al., 2020; Bae et al., 2018; Prokes and Hlozek, 2007; Sapozhnikova and Hoh, 2019; Xu et al., 2019). Among these, 2-methylanthracene has been confirmed as an AhR-binding compound based on results from H4IIE-*luc* bioassays (Larsson et al., 2014). In addition, 9-methylanthracene was shown to bind and activate AhR in H4IIE. GudLuc1.1 cell assays (Vondráček et al., 2007). Triphenylmethane, detected in all samples with the highest peak intensity, is a widely used dye precursor in the textile, paper, and pharmaceutical industries (Upadhyay et al., 2023). Its complex aromatic structure confers strong resistance to biodegradation, contributing to its environmental persistence and poor removal during sewage treatment, posing ecological risks through effluent discharge (Upadhyay et al., 2023). Other detected compounds include *o*-terphenyl, used in high-temperature industrial applications (Mansi et al., 2021), and 1,1,3,3-tetraphenyl-1,3-dimethyldisiloxane, a silicone-based compound likely derived from nearby industrial activity (Itoh and Yang, 2002). Abietatriene, a naturally occurring diterpene, was also identified and is known to originate from plant sources (Fan et al., 2017). In contrast, limited information is available on the toxicity, origin, and environmental behavior of compounds such as 4-cyclohexylbiphenyl and phthalic acid, 3,5-dimethylphenyl 3-methylphenyl ester. Meanwhile, the significant AhR activity observed in the F3 fraction of fish extracts underscores the need for future studies employing LC-QTOFMS-based nontarget screening to investigate polar substances with potentially high bioavailability in aquatic organisms. This is particularly relevant for fish inhabiting urban river systems, where frequent exposure to wastewater discharges is common. Such hydrophilic contaminants, often originating from STP effluents, may represent emerging environmental concerns.

3.7. Prediction of additional toxicities of AhR agonist candidates

VirtualToxLab in silico modeling was employed to predict the AhR binding affinity of the 19 identified AhR agonist candidates (Fig. 4c and Table S10). The results indicated that all candidates have the potential to bind to AhR. Notably, 7-isopropyl-1-methyl-1,2,3,4-tetrahydrophenanthrene, 10,18-bisnorabieta-8,11,13-triene, dehydroabietine, triphenylmethane, *o*-terphenyl, 1,1,3,3-tetraphenyl-1,3-dimethyldisiloxane, and 4-cyclohexylbiphenyl were predicted to exhibit stronger AhR binding affinity than the reference compound BaP. Moreover, most candidates showed higher toxic potential scores than previously reported target AhR agonists, which ranged from 0.367 to 0.474 (Gwak et al., 2024). Given their high peak intensities in the extracts (Henderson et al., 2009; Ieda et al., 2019; Liu et al., 2024), these compounds are likely contributors to the observed AhR-mediated responses. Nonetheless, toxicological validation and chemical confirmation are necessary to substantiate their AhR activity.

Environmental pollutants may interact not only with the AhR but also with other molecular targets, potentially leading to a range of biological effects (Hashmi et al., 2020; Whirledge et al., 2015). Chronic exposure to such compounds can result in developmental toxicity and population-level impacts in fish (Segner et al., 2021; Tian et al., 2021). In addition to AhR, the potential for these compounds to interact with other hormone receptors, including AR, ER, GR, and TR, was also assessed using VirtualToxLab (Table S10). The predicted toxic potentials toward these endocrine receptors were generally low and significantly lower than their affinities for AhR. Despite the relatively low predicted binding affinities to hormone receptors, there remains a potential risk of endocrine disruption arising from combined effects across multiple signaling pathways. A cumulative toxicity ranking based on total predicted receptor activity revealed triphenylmethane as the most toxic

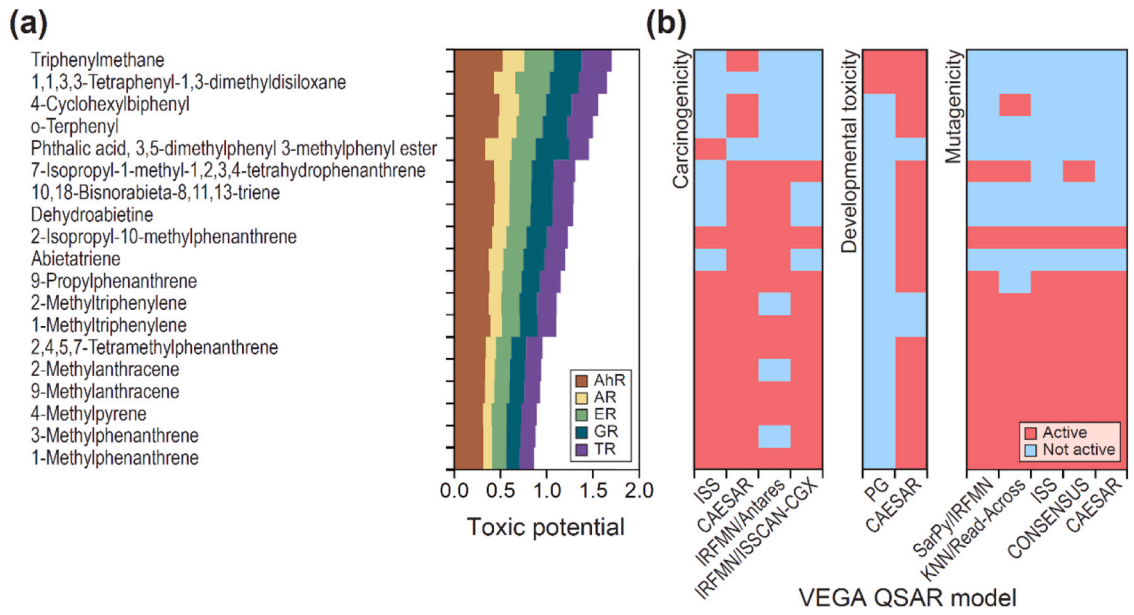

Fig. 5. Predicted potential toxicological profiles of the 19 AhR agonist candidates detected in fish. (a) Toxic potential toward AhR and other hormone receptors (i.e., AR, ER, GR, and TR) assessed using VirtualToxLab. (b) Predicted carcinogenicity, developmental toxicity, and mutagenicity evaluated using VEGA QSAR models.

compound, followed by 1,1,3,3-tetraphenyl-1,3-dimethyldisiloxane and 4-cyclohexylbiphenyl (Fig. 5a). These substances may accumulate in the Gapcheon River ecosystem, posing potential ecological risks to aquatic organisms. Further toxicity predictions were performed using the VEGA QSAR models (Fig. 5b and Table S11). All but one compound were predicted to be potentially carcinogenic. Regarding developmental toxicity, all compounds except phthalic acid, 3,5-dimethylphenyl 3-methylphenyl ester, 2-methyltriphenylene, and 1-methyltriphenylene were predicted to be active. Approximately half of the compounds were also predicted to be mutagenic. Notably, the compounds identified as toxic by VEGA did not fully align with those ranked highest in VirtualToxLab, suggesting that different models capture distinct facets of chemical toxicity. These findings contribute to the prioritization of hazardous compounds and support the development of effect-based screening frameworks and long-term monitoring strategies for aquatic environments. Their presence in freshwater fish and the potential for multiple toxic effects underscore their ecological relevance and the need to assess their broader impact on biodiversity and trophic dynamics within the Gapcheon River ecosystem.

4. Conclusions

This study investigated the distribution and composition of PTSs in various organs of freshwater fish across different trophic levels in the Gapcheon River, an urban waterway in South Korea. To complement traditional chemical analysis, we employed the EDA approach to identify major AhR agonists in fish tissues. The results highlight the need for regulatory attention to specific compounds such as BbA, which may pose ecotoxicological risks in freshwater ecosystems. In addition, NTS identified AhR agonist candidates in fish associated with urban and industrial sources. These compounds are likely derived from nonpoint sources, industrial discharge, and incomplete removal in STP, leading to their release into the river and subsequent accumulation in fish. While limitations such as small sample size and variations among different tissues may have introduced variability in the distribution patterns observed. The detection of these substances indicates their potential role as biological stressors, posing risks to aquatic organisms and potentially disrupting the ecological balance of freshwater ecosystems. These findings underscore the need for further research to clarify the sources, environmental fate, and ecotoxicological impacts of AhR agonists, particularly those linked to STP effluents, industrial activities, and environmental transport mechanisms.

CRediT authorship contribution statement

Seongjin Hong: Writing – review & editing, Visualization, Supervision, Project administration, Investigation, Funding acquisition, Formal analysis, Conceptualization. **Jiyun Gwak:** Investigation, Formal analysis, Data curation. **Jihyun Cha:** Writing – original draft, Visualization, Investigation, Formal analysis, Data curation, Conceptualization. **Kyung-Hoon Shin:** Writing – review & editing, Investigation, Formal analysis. **Eun-Ji Won:** Investigation, Formal analysis. **Dokyun Kim:** Investigation, Formal analysis, Data curation. **Junghyun Lee:** Writing – review & editing, Formal analysis, Data curation. **Jong Seong Khim:** Writing – review & editing, Methodology, Formal analysis, Conceptualization. **Hyo-Bang Moon:** Writing – review & editing, Formal analysis, Data curation.

Declaration of Competing Interest

The authors declare that they have no known competing financial interests or personal relationships that could have appeared to influence the work reported in this paper.

Acknowledgments

This research was supported by the Korean Institute of Marine Science & Technology Promotion (KIMST), funded by the Ministry of Oceans and Fisheries (RS-2022-KS221655 and RS-2024-00417889). This research was also supported by a grant from the National Research Foundation of Korea (NRF) (RS-2021-NR061341).

Appendix A. Supporting information

Supplementary data associated with this article can be found in the online version at doi:10.1016/j.ecoenv.2025.118579.

Data availability

Data will be made available on request.

References

An, Y., Hong, S., Kim, Y., Kim, M., Choi, B., Won, E.-J., Shin, K.-H., 2020. Trophic transfer of persistent toxic substances through a coastal food web in Ulsan Bay, South Korea: application of compound-specific isotope analysis of nitrogen in amino acids. Environ. Pollut. 266, 115160. https://doi.org/10.1016/j.envpol.2020.115160.

Bae, M.-S., Park, J.K., Kim, K.-H., Cho, S.-S., Lee, K.-Y., Shon, Z.-H., 2018. Emission and cytotoxicity of surgical smoke: cholesta-3,5-diene released from pyrolysis of prostate tissue. Atmosphere 9, 381. https://doi.org/10.3390/atmos9100381.

Bak, S.-M., Nakata, H., Koh, D.-H., Yoo, J., Iwata, H., Kim, E.-Y., 2019. In vitro and in silico AHR assays for assessing the risk of heavy oil-derived polycyclic aromatic hydrocarbons in fish. Ecotox. Environ. Safe 181, 214–223. https://doi.org/10.1016/j.ecoenv.2019.06.008.

Baumard, P., Budzinski, H., Garrigues, P., Sorbe, J.C., Burgeot, T., Bellocq, J., 1998. Concentrations of PAHs (polycyclic aromatic hydrocarbons) in various marine organisms in relation to those in sediments and to trophic level. Mar. Pollut. Bull. 36, 951–960. https://doi.org/10.1016/S0025-326X(98)00088-5.

Bik, E., Ishigaki, M., Blat, A., Jasztal, A., Ozaki, Y., Malek, K., Baranska, M., 2020. Lipid Droplet composition varies based on medaka fish eggs development as revealed by NIR-, MIR-, and Raman imaging. Molecules 25, 817. https://doi.org/10.3390/molecules25040817.

Bittarello, A.C., Vieira, J.C.S., Braga, C.P., da Cunha Bataglioli, I., de Oliveira, G., Rocha, L.C., Zara, L.F., Buzalaf, M.A.R., de Oliveira, L.C.S., Adamec, J., de Magalhães Padilha, P., 2020. Metalloproteomic approach of mercury-binding proteins in liver and kidney tissues of Plagioscion squamosissimus (corvina) and Colossoma macropomum (tambaqui) from Amazon region: possible identification of mercury contamination biomarkers. Sci. Total Environ. 711, 134547. https://doi.org/10.1016/j.scitotenv.2019.134547.

Black, G.P., He, G., Denison, M.S., Young, T.M., 2021. Using estrogenic activity and nontargeted chemical analysis to identify contaminants in sewage sludge. Environ. Sci. Technol. 55, 6729–6739. https://doi.org/10.1021/acs.est.0c07846.

Blanke, C.M., Chikaraishi, Y., Takizawa, Y., Steffan, S.A., Dharampal, P.S., Vander Zanden, M.J., 2017. Comparing compound-specific and bulk stable nitrogen isotope trophic discrimination factors across multiple freshwater fish species and diets. Can. J. Fish. Aquat. Sci. 74, 1291–1297. https://doi.org/10.1139/cjfas-2016-0420.

Bocio, A., Domingo, J.L., Falcó, G., Llobet, J.M., 2007. Concentrations of PCDD/PCDFs and PCBs in fish and seafood from the Catalan (Spain) market: estimated human intake. Environ. Int. 33, 170–175. https://doi.org/10.1016/j.envint.2006.09.005.

Brack, W., 2003. Effect-directed analysis: a promising tool for the identification of organic toxicants in complex mixtures? Anal. Bional. Chem. 377, 397–407. https://doi.org/10.1007/s00216-003-2139-z.

Brack, W., Ait-Aissa, S., Burgess, R.M., Busch, W., Creusot, N., Di Paolo, C., Escher, B.I., Mark Hewitt, L., Hilscherova, K., Hollender, J., Hollert, H., Jonker, W., Kool, J., Lamoree, M., Muschket, M., Neumann, S., Rostkowski, P., Ruttkies, C., Schollee, J., Schymanski, E.L., Schulze, T., Seiler, T.-B., Tindall, A.J., De Aragão Umbuzeiro, G., Vrana, B., Krauss, M., 2016. Effect-directed analysis supporting monitoring of aquatic environments — an in-depth overview. Sci. Total Environ. 544, 1073–1118. https://doi.org/10.1016/j.scitotenv.2015.11.102.

Cambiaghi, A., Ferrario, M., Masseroli, M., 2017. Analysis of metabolomic data: tools, current strategies and future challenges for omics data integration. Brief. Bioinform 18, 498–510. https://doi.org/10.1093/bib/bbw031.

Cha, J., Hong, S., Gwak, J., Kim, M., Lee, J., Kim, T., Han, G.M., Hong, S.H., Hur, J., Giesy, J.P., Khim, J.S., 2022. Identification of novel polar aryl hydrocarbon receptor agonists accumulated in liver of black-tailed gulls in Korea using advanced effect-directed analysis. J. Hazard. Mater. 429, 128305. https://doi.org/10.1016/j.jhazmat.2022.128305.

Cha, J., Hong, S., Kim, J., Lee, J., Yoon, S.J., Lee, S., Moon, H.-B., Shin, K.-H., Hur, J., Giesy, J.P., Khim, J.S., 2019. Major AhR-active chemicals in sediments of Lake Sihwa, South Korea: application of effect-directed analysis combined with full-scan screening analysis. Environ. Int. 133, 105199. https://doi.org/10.1016/j.envint.2019.105199.

Cha, J., Hong, S., Lee, J., Gwak, J., Kim, M., Kim, T., Hur, J., Giesy, J.P., Khim, J.S., 2021. Novel polar AhR-active chemicals detected in sediments of an industrial area using effect-directed analysis based on in vitro bioassays with full-scan high resolution mass spectrometric screening. Sci. Total Environ. 779, 146566. https://doi.org/10.1016/j.scitotenv.2021.146566.

Cha, J., Hong, S., Lee, J., Gwak, J., Kim, M., Mok, S., Moon, H.-B., Jones, P.D., Giesy, J.P., Khim, J.S., 2023. Identification of mid-polar and polar AhR agonists in cetaceans from Korean Coastal waters: application of effect-directed analysis with full-scan screening. Environ. Sci. Technol. 57, 15644–15655. https://doi.org/10.1021/acs.est.3c04311.

Cheng, F., Escher, B.I., Li, H., König, M., Tong, Y., Huang, J., He, L., Wu, X., Lou, X., Wang, D., Wu, F., Pei, Y., Yu, Z., Brooks, B.W., Zeng, E.Y., You, J., 2024. Deep learning bridged bioactivity, structure, and GC-HRMS-readable evidence to decipher nontarget toxicants in sediments. Environ. Sci. Technol. 58, 15415–15427. https://doi.org/10.1021/acs.est.3c10814.

Cheung, K.C., Leung, H.M., Kong, K.Y., Wong, M.H., 2007. Residual levels of DDTs and PAHs in freshwater and marine fish from Hong Kong markets and their health risk assessment. Chemosphere 66, 460–468. https://doi.org/10.1016/j.chemosphere.2006.06.008.

Chikaraishi, Y., Ogawa, N.O., Kashiyama, Y., Takano, Y., Suga, H., Tomitani, A., Miyashita, H., Kitazato, H., Ohkouchi, N., 2009. Determination of aquatic food-web structure based on compound-specific nitrogen isotopic composition of amino acids. Limnol. Oceanogr. Methods 7, 740–750. https://doi.org/10.4319/lom.2009.7.740.

Connon, R.E., Geist, J., Werner, I., 2012. Effect-based tools for monitoring and predicting the ecotoxicological effects of chemicals in the aquatic environment. Sensors 12, 12741–12771. https://doi.org/10.3390/s120912741.

van der Oost, R., Beyer, J., Vermeulen, N.P.E., 2003. Fish bioaccumulation and biomarkers in environmental risk assessment: a review. Environ. Toxicol. Phar 13, 57–149. https://doi.org/10.1016/S1382-6689(02)00126-6.

Doering, J.A., Wiseman, S., Beitel, S.C., Tendler, B.J., Giesy, J.P., Hecker, M., 2012. Tissue specificity of aryl hydrocarbon receptor (AhR) mediated responses and relative sensitivity of white sturgeon (*Acipenser transmontanus*) to an AhR agonist. Aquat. Toxicol. 114–115, 125–133. https://doi.org/10.1016/j.aquatox.2012.02.015.

Driscoll, C.T., Mason, R.P., Chan, H.M., Jacob, D.J., Pirrone, N., 2013. Mercury as a global pollutant: sources, pathways, and effects. Environ. Sci. Technol. 47, 4967–4983.

Du, Y., Xu, X., Liu, Q., Bai, L., Hang, K., Wang, D., 2022. Identification of organic pollutants with potential ecological and health risks in aquatic environments: progress and challenges. Sci. Total Environ. 806, 150691. https://doi.org/10.1021/es305071v.

Escher, B.I., Stapleton, H.M., Schymanski, E.L., 2020. Tracking complex mixtures of chemicals in our changing environment. Science 367, 388–392. https://doi.org/10.1126/science.aay6636.

Escher, B.I., Stapleton, H.M., Schymanski, E.L., 2020. Tracking complex mixtures of chemicals in our changing environment. Science 367, 388–392. https://doi.org/10.1126/science.aay6636.

Fan, D., Zhou, S., Zheng, Z., Zhu, G.-Y., Yao, X., Yang, M.-R., Jiang, Z.-H., Bai, L.-P., 2017. New Abietane and Kaurane Type Diterpenoids from the Stems of Tripterygium regelii. Int. J. Mol. Sci. 18, 147. https://doi.org/10.3390/ijms18010147.

Flesher, J.W., Lehner, A.F., 2016. Structure, function and carcinogenicity of metabolites of methylated and non-methylated polycyclic aromatic hydrocarbons: a comprehensive review. Toxicol. Mech. Method 26, 151–179. https://doi.org/10.3109/15376516.2015.1135223.

Gwak, J., Cha, J., Lee, J., Kim, Y., An, S.-A., Lee, S., Moon, H.-B., Hur, J., Giesy, J.P., Hong, S., Khim, J.S., 2022a. Effect-directed identification of novel aryl hydrocarbon receptor-active aromatic compounds in coastal sediments collected from a highly industrialized area. Sci. Total Environ. 803, 149969. https://doi.org/10.1016/j.scitotenv.2021.149969.

Gwak, J., Cha, J., Nam, S.-I., Kim, J.-H., Lee, J., Moon, H.-B., Khim, J.S., Hong, S., 2024. Characterization of AhR-mediated potency in sediments from Kongsfjorden, Svalbard: application of effect-directed analysis and nontarget screening. Chemosphere 368, 143771. https://doi.org/10.1016/j.chemosphere.2024.143771.

Gwak, J., Lee, J., Cha, J., Kim, M., Hur, J., Cho, J., Kim, M.S., Jang, K.-S., Giesy, J.P., Hong, S., Khim, J.S., 2022b. Molecular characterization of estrogen receptor agonists during sewage treatment processes using effect-directed analysis combined with high-resolution full-scan screening. Environ. Sci. Technol. 56, 13085–13095. https://doi.org/10.1021/acs.est.2c03428.

Hansen, B.H., Nordtug, T., Øverjordet, I.B., Sørensen, L., Kvæstad, B., Davies, E.J., Meier, S., Gomes, T., Brooks, S., Farkas, J., 2022. Monitoring ocean water quality by deployment of lumpfish (*Cyclopterus lumpus*) eggs: in situ bioaccumulation and toxicity in embryos. Ecotox. Environ. Safe. 245, 114074. https://doi.org/10.1016/j.ecoenv.2022.114074.

Hashmi, M.A.K., Krauss, M., Escher, B.I., Teodorovic, I., Brack, W., 2020. Effect-directed analysis of progestogens and glucocorticoids at trace concentrations in river water. Environ. Toxicol. Chem. 39, 189–199. https://doi.org/10.1002/etc.4609.

Henderson, R.K., Baker, A., Murphy, K.R., Hambly, A., Stuetz, R.M., Khan, S.J., 2009. Fluorescence as a potential monitoring tool for recycled water systems: a review. Water Res 43, 863–881. https://doi.org/10.1016/j.watres.2008.11.027.

Hong, S., Giesy, J.P., Lee, J.-S., Lee, J.-H., Khim, J.S., 2016. Effect-directed analysis: current status and future challenges. Ocean Sci. J. 51, 413–433. https://doi.org/10.1007/s12601-016-0038-4.

Hong, S., Lee, J., Cha, J., Gwak, J., Khim, J.S., 2023. Effect-directed analysis combined with nontarget screening to identify unmonitored toxic substances in the environment. Environ. Sci. Technol. 57, 19148–19155. https://doi.org/10.1021/acs.est.3c05035.

Hu, J., Lyu, Y., Chen, H., Li, S., Sun, W., 2023. Suspect and nontarget screening reveal the underestimated risks of antibiotic transformation products in wastewater treatment plant effluents. Environ. Sci. Technol. 57, 17439–17451. https://doi.org/10.1021/acs.est.3c05008.

Huang, M., Mesaros, C., Hackfeld, L.C., Hodge, R.P., Blair, I.A., Penning, T.M., 2017. Potential metabolic activation of representative alkylated polycyclic aromatic hydrocarbons 1-methylphenanthrene and 9-ethylphenanthrene associated with the deepwater horizon oil spill in human hepatoma (HepG2) cells. Chem. Res. Toxicol. 30, 2140–2150. https://doi.org/10.1021/acs.chemrestox.7b00232.

Ieda, T., Hashimoto, S., Isobe, T., Kunisue, T., Tanabe, S., 2019. Evaluation of a data-processing method for target and non-target screening using comprehensive two-dimensional gas chromatography coupled with high-resolution time-of-flight mass spectrometry for environmental samples. Talanta 194, 461–468. https://doi.org/10.1016/j.talanta.2018.10.050.

Itoh, T., Yang, M.-H., 2002. Temperature dependence of the fluorescence quantum yields of diphenylsiloxane-based copolymers in dilute solutions. J. Polym. Sci. Pol. Phys. 40, 854–861. https://doi.org/10.1002/polb.10151.

Jang, Y., Son, B., Chu, S., Lim, B., 2019. Characteristics and management plan of water quality at the water pollution deterioration area of the upper stream of Gapcheon. J. Korean Soc. Water Environ. 35, 399–408.

Jordan-Ward, R., von Hippel, F.A., Zheng, G., Salamova, A., Dillon, D., Gologergen, J., Immingan, T., Dominguez, E., Miller, P., Carpenter, D., Postlethwait, J.H., Byrne, S., Buck, C.L., 2022. Elevated mercury and PCB concentrations in Dolly Varden

(Salvelinus malma) collected near a formerly used defense site on Sivuqaq, Alaska. Sci. Total Environ. 826, 154067. https://doi.org/10.1016/j.scitotenv.2022.154067.
Kelly, B.C., Ikonomou, M.G., Blair, J.D., Morin, A.E., Gobas, F.A.P.C., 2007. Food web–specific biomagnification of persistent organic pollutants. Science 317, 236–239. https://doi.org/10.1126/science.1138275.
Kidd, K.A., Bootsma, H.A., Hesslein, R.H., Lyle Lockhart, W., Hecky, R.E., 2003. Mercury concentrations in the food web of Lake Malawi, East Africa. J. Gt. Lakes Res 29, 258–266. https://doi.org/10.1016/S0380-1330(03)70553-X.
Kim, D., Cho, H.-E., Won, E.J., Kim, H.-J., Lee, S., An, K.-G., Moon, H.-B., Shin, K.H., 2022. Environmental fate and trophic transfer of synthetic musk compounds and siloxanes in Geum River, Korea: compound-specific nitrogen isotope analysis of amino acids for accurate trophic position estimation. Environ. Int. 161, 107123. https://doi.org/10.1016/j.envint.2022.107123.
Kim, J., Hong, S., Cha, J., Lee, J., Kim, T., Lee, S., Moon, H.-B., Shin, K.-H., Hur, J., Lee, J.-S., Giesy, J.P., Khim, J.S., 2019. Newly identified AhR-active compounds in the sediments of an industrial area using effect-directed analysis. Environ. Sci. Technol. 53, 10043–10052. https://doi.org/10.1021/acs.est.9b02166.
Kim, C.-K., Lee, T.-W., Lee, K.-T., Lee, J.-H., Lee, C.-B., 2012. Nationwide monitoring of mercury in wild and farmed fish from fresh and coastal waters of Korea. Chemosphere 89, 1360–1368. https://doi.org/10.1016/j.chemosphere.2012.05.093.
Kim, D., Won, E.-J., Cho, H.-E., Jo, H.-W., Choi, K.-Y., Kim, C.-J., Shin, K.-H., 2025. Probabilistic Trophic Magnification Analysis for Assessing the Bioaccumulation Potential of Organophosphate Flame Retardants in Freshwater Ecosystems of South Korea. Ecotox. Environ. Safe. (In revision).
Koehn, J.D., 2004. Carp (*Cyprinus carpio*) as a powerful invader in Australian waterways. Freshw. Biol. 49, 882–894. https://doi.org/10.1111/j.1365-2427.2004.01232.x.
Koh, C.H., Khim, J.S., Kannan, K., Villeneuve, D.L., Senthilkumar, K., Giesy, J.P., 2004. Polychlorinated dibenzo-p-dioxins (PCDDs), dibenzofurans (PCDFs), biphenyls (PCBs), and polycyclic aromatic hydrocarbons (PAHs) and 2,3,7,8-TCDD equivalents (TEQs) in sediment from the Hyeongsan River, Korea. Environ. Pollut. https://doi.org/10.1016/j.envpol.2004.05.001.
Koistinen, J., Lehtonen, M., Tukia, K., Soimasuo, M., Lahtiperä, M., Oikari, A., 1998. Identification of lipophilic pollutants discharged from a finnish pulp and paper mill. Chemosphere 37, 219–235. https://doi.org/10.1016/S0045-6535(98)00041-1.
Larsson, M., Hagberg, J., Giesy, J.P., Engwall, M., 2014. Time-dependent relative potency factors for polycyclic aromatic hydrocarbons and their derivatives in the H4IIE-luc bioassay. Environ. Toxicol. Chem. 33, 943–953. https://doi.org/10.1002/etc.2517.
Lee, J., Hong, S., Kim, T., Park, S.Y., Cha, J., Kim, Y., Gwak, J., Lee, S., Moon, H.-B., Hu, W., Wang, T., Giesy, J.P., Khim, J.S., 2022. Identification of AhR agonists in sediments of the Bohai and Yellow Seas using advanced effect-directed analysis and in silico prediction. J. Hazard. Mater. 435, 128908. https://doi.org/10.1016/j.jhazmat.2022.128908.
Lee, K.T., Hong, S., Lee, J.S., Chung, K.H., Hilscherová, K., Giesy, J.P., Khim, J.S., 2013. Revised relative potency values for PCDDs, PCDFs, and non-ortho-substituted PCBs for the optimized H4IIE-luc in vitro bioassay. Environ. Sci. Pollut. R. 20, 8590–8599. https://doi.org/10.1007/s11356-013-1770-2.
Lee, Y.M., Kim, K.S., Jacobs Jr, D.R., Lee, D.H., 2017. Persistent organic pollutants in adipose tissue should be considered in obesity research. Obes. Rev. 18, 129–139. https://doi.org/10.1111/obr.12481.
Li, M., Ellis, G.S., 2015. Qualitative and quantitative analysis of dibenzofuran, alkyldibenzofurans, and benzo[b]naphthofurans in crude oils and source rock Extracts. Energ. Fuel 29, 1421–1430. https://doi.org/10.1021/ef502558a.
Lille-Langøy, R., Jørgensen, K.B., Goksøyr, A., Pampanin, D.M., Sydnes, M.O., Karlsen, O. A., 2021. Substituted two- to five-ring polycyclic aromatic compounds are potent agonists of atlantic cod (*Gadus morhua*) aryl hydrocarbon receptors Ahr1a and Ahr2a. Environ. Sci. Technol. 55, 15123–15135. https://doi.org/10.1021/acs.est.1c02946.
Listrat, A., Lebret, B., Louveau, I., Astruc, T., Bonnet, M., Lefaucheur, L., Picard, B., Bugeon, J., 2016. How muscle structure and composition influence meat and flesh quality. Sci. World J. 2016, 3182746. https://doi.org/10.1155/2016/3182746.
Liu, H., Wang, R., Zhao, B., Xie, D., 2024. Assessment for the data processing performance of non-target screening analysis based on high-resolution mass spectrometry. Sci. Total Environ. 908, 167967. https://doi.org/10.1016/j.scitotenv.2023.167967.
Lorrain, A., Savoye, N., Chauvaud, L., Paulet, Y.-M., Naulet, N., 2003. Decarbonation and preservation method for the analysis of organic C and N contents and stable isotope ratios of low-carbonated suspended particulate material. Anal. Chim. Acta 491, 125–133. https://doi.org/10.1016/S0003-2670(03)00815-8.
Mansi, E., Sau, S., Balog, I., Caputo, G., Corsaro, N., Tiranti, G., Filippi, F., Panza, F., Ratto, N., Simonetti, A., Tizzoni, A.C., Ciotti, M., Cemmi, A., Annesini, M.C., 2021. High temperature stability of a commercial terphenyl-based thermal oil. Prog. Nucl. Energ. 140, 103900. https://doi.org/10.1016/j.pnucene.2021.103900.
Marzo, M., Kulkarni, S., Manganaro, A., Roncaglioni, A., Wu, S., Barton-Maclaren, T.S., Lester, C., Benfenati, E., 2016. Integrating in silico models to enhance predictivity for developmental toxicity. Toxicology 370, 127–137. https://doi.org/10.1016/j.tox.2016.09.015.
Masunaga, S., Sakashita, R., Furuichi, T., Shirai, J., Kannan, K., Giesy, J., 2004. Effect of exposure duration on the aryl hydrocarbon receptor-mediated activity of polycyclic aromatic hydrocarbons measured by in vitro reporter gene assay. Organomet. Compd. 66, 623–629.
Mekenyan, O.G., Veith, G.D., Call, D.J., Ankley, G.T., 1996. A QSAR evaluation of Ah receptor binding of halogenated aromatic xenobiotics. Environ. Health Persp 104, 1302–1310. https://doi.org/10.1289/ehp.961041302.
Minagawa, M., Wada, E., 1984. Stepwise enrichment of ^{15}N along food chains: Further evidence and the relation between δ15N and animal age. Geochim. Cosmochim. Acta 48, 1135–1140. https://doi.org/10.1016/0016-7037(84)90204-7.
Mok, S., Lee, S., Choi, Y., Jeon, J., Kim, Y.H., Moon, H.-B., 2023. Target and non-target analyses of neutral per- and polyfluoroalkyl substances from fluorochemical industries using GC-MS/MS and GC-TOF: insights on their environmental fate. Environ. Int. 182, 108311. https://doi.org/10.1016/j.envint.2023.108311.
Mok, S., Lee, S., Lee, N., Kim, S., Choi, K., Park, J., Kho, Y., Moon, H.-B., 2024. Nationwide human biomonitoring strategy in Korea: prioritization of novel contaminants using GC/TOF-MS with suspect and non-target screening. Chemosphere 369, 143814. https://doi.org/10.1016/j.chemosphere.2024.143814.
Moon, J.Y., Kim, Y.B., Lee, S.I., Song, H., Choi, K., Jeong, G.H., 2006. Distribution characteristics of polychlorinated biphenyls in crucian carp (*Carassius auratus*) from major rivers in Korea. Chemosphere 62, 430–439. https://doi.org/10.1016/j.chemosphere.2005.04.063.
Muz, M., Krauss, M., Kutsarova, S., Schulze, T., Brack, W., 2017. Mutagenicity in surface waters: synergistic effects of carboline alkaloids and aromatic amines. Environ. Sci. Technol. 51, 1830–1839. https://doi.org/10.1021/acs.est.6b05468.
Nagpal, N., 1993. Ambient water quality criteria for polycyclic aromatic hydrocarbons (PAHs), BC. Environ. Water Qual. Branch.
Ndabambi, M., Kim, K.Y., Jung, J.-H., Yim, U.-H., Oh, J.-E., 2021. Alkylated phenanthrene distributions in black rockfish (*Sebastes schlegelii*) and biotransformation into hydroxylated metabolites after intragastric administration. Sci. Total Environ. 762, 143160. https://doi.org/10.1016/j.scitotenv.2020.143160.
Neale, P.A., Escher, B.I., de Baat, M.L., Dechesne, M., Dingemans, M.M.L., Enault, J., Pronk, G.J., Smeets, P.W.M.H., Leusch, F.D.L., 2023. Application of effect-based methods to water quality monitoring: answering frequently asked questions by water quality managers, regulators, and policy makers. Environ. Sci. Technol. 57, 6023–6032. https://doi.org/10.1021/acs.est.2c06365.
Neff, J., 1979. Polycyclic Aromatic Hydrocarbons Sources Fates and Biological Effects. Applied Science Publ, London, p. 262.
Ogbesejana, A.B., Sonibare, O.O., Ningning, Z., 2019. Occurrence and distribution of pyrene and its derivatives in crude oils and source rock extracts from Niger Delta. Niger. J. Pet. Technol. 9, 3–17.
Oikari, A., Fragoso, N., Leppänen, H., Chan, T., Hodson, P.V., 2002. Bioavailability to juvenile rainbow trout (Oncorynchus mykiss) of retene and other mixed-function oxygenase-active compounds from sediments. Environ. Toxicol. Chem. 21, 121–128. https://doi.org/10.1002/etc.5620210118.
Ololade, I.A., Apata, A.O., Alabi, B.A., Akindumila, O.I., Oloyede, O.J., Obasusi, B.A., 2024. Polycyclic aromatic hydrocarbons (PAHs) in fish (*Clarias gariepinus*) of southwestern rivers. In: Reg. Stud. Mar. Sci., 77. Occurrence, distribution, and potential human exposure risks, Nigeria, 103687. https://doi.org/10.1016/j.rsma.2024.103687.
Park, T.-J., Kim, M.-K., Lee, S.-H., Lee, Y.-S., Kim, M.-J., Song, H.-Y., Park, J.-H., Zoh, K.-D., 2022. Occurrence and characteristics of microplastics in fish of the Han River, South Korea: Factors affecting microplastic abundance in fish. Environ. Res. 206, 112647. https://doi.org/10.1016/j.envres.2021.112647.
Phillips, A.L., Williams, A.J., Sobus, J.R., Ulrich, E.M., Gundersen, J., Langlois-Miller, C., Newton, S.R., 2022. A framework for utilizing high-resolution mass spectrometry and nontargeted analysis in rapid response and emergency situations. Environ. Toxicol. Chem. 41, 1117–1130. https://doi.org/10.1002/etc.5196.
Price, E.R., Mager, E.M., 2020. The effects of exposure to crude oil or PAHs on fish swim bladder development and function. Comp. Biochem. Phys. C. 238, 108853. https://doi.org/10.1016/j.cbpc.2020.108853.
Prokes, L., Hlozek, M., 2007. Identification of some adhesives and wood pyrolysis products of archaeological origin by direct inlet mass spectrometry. Chem. Anal. 52, 700–713.
Qadeer, A., Liu, M., Yang, J., Liu, X., Khalil, S.K., Huang, Y., Habibullah-Al-Mamun, M., Gao, D., Yang, Y., 2019. Trophodynamics and parabolic behaviors of polycyclic aromatic hydrocarbons in an urbanized lake food web, Shanghai. Ecotoxicol. Environ. Safe 178, 17–24. https://doi.org/10.1016/j.ecoenv.2019.04.003.
Qin, N., He, W., Liu, W., Kong, X., Xu, F., Giesy, J.P., 2020. Tissue distribution, bioaccumulation, and carcinogenic risk of polycyclic aromatic hydrocarbons in aquatic organisms from Lake Chaohu, China. Sci. Total Environ. 749, 141577. https://doi.org/10.1016/j.scitotenv.2020.141577.
Ramdahl, T., 1983. Retene—a molecular marker of wood combustion in ambient air. Nature 306, 580–582. https://doi.org/10.1038/306580a0.
Ruan, T., Li, P., Wang, H., Li, T., Jiang, G., 2023. Identification and prioritization of environmental organic pollutants: from an analytical and toxicological perspective. Chem. Rev. 123, 10584–10640. https://doi.org/10.1021/acs.chemrev.3c00056.
Rude, C.I., Wilson, L.B., La Du, J., Lalli, P.M., Colby, S.M., Schultz, K.J., Smith, J.N., Waters, K.M., Tanguay, R.L., 2024. Aryl hydrocarbon receptor-dependent toxicity by retene requires metabolic competence. Toxicol. Sci. 202, 50–68. https://doi.org/10.1093/toxsci/kfae098.
Russell, R.W., Gobas, F.A.P.C., Haffner, G.D., 1999. Maternal transfer and in ovo exposure of organochlorines in oviparous organisms: a model and field verification. Environ. Sci. Technol. 33, 416–420. https://doi.org/10.1021/es9800737.
Sapozhnikova, Y., Hoh, E., 2019. Suspect screening of chemicals in food packaging plastic film by comprehensive two-dimensional gas chromatography coupled to time-of-flight mass spectrometry. LC GC N. Am. 37, 52–65.
Schaupp, C.M., Maloney, E.M., Mattingly, K.Z., Olker, J.H., Villeneuve, D.L., 2023. Comparison of in silico, in vitro, and in vivo toxicity benchmarks suggests a role for ToxCast data in ecological hazard assessment. Toxicol. Sci. 195, 145–154. https://doi.org/10.1093/toxsci/kfad072.

Segner, H., Bailey, C., Tafalla, C., Bo, J., 2021. Immunotoxicity of xenobiotics in fish: a role for the aryl hydrocarbon receptor (AhR). ? Int. Int. J. Mol. Sci. 22, 9460. https://doi.org/10.3390/ijms22179460.

Simon, E., van Velzen, M., Brandsma, S.H., Lie, E., Løken, K., de Boer, J., Bytingsvik, J., Jenssen, B.M., Aars, J., Hamers, T., Lamoree, M.H., 2013. Effect-directed analysis to explore the polar bear exposome: identification of thyroid hormone disrupting compounds in plasma. Environ. Sci. Technol. 47, 8902–8912. https://doi.org/10.1021/es401696u.

Snyder, S.M., Pulster, E.L., Wetzel, D.L., Murawski, S.A., 2015. PAH exposure in Gulf of Mexico demersal fishes, post-deepwater horizon. Environ. Sci. Technol. 49, 8786–8795. https://doi.org/10.1021/acs.est.5b01870.

Sun, Y., Miller, C.A., III, Wiese, T.E., Blake, D.A., 2014. Methylated phenanthrenes are more potent than phenanthrene in a bioassay of human aryl hydrocarbon receptor (AhR) signaling. Environ. Toxicol. Chem. 33, 2363–2367. https://doi.org/10.1002/etc.2687.

Sun, Y., Yu, H., Zhang, J., Yin, Y., Shi, H., Wang, X., 2006. Bioaccumulation, depuration and oxidative stress in fish *Carassius auratus* under phenanthrene exposure. Chemosphere 63, 1319–1327. https://doi.org/10.1016/j.chemosphere.2005.09.032.

Suzuki, G., Takigami, H., Kushi, Y., Sakai, S.-i, 2006. Time-course changes of mixture effects on AhR binding-dependent luciferase activity in a crude extract from a compost sample. Toxicol. Lett. 161, 174–187. https://doi.org/10.1016/j.toxlet.2005.09.004.

Tian, Z., Zhao, H., Peter, K.T., Gonzalez, M., Wetzel, J., Wu, C., Hu, X., Prat, J., Mudrock, E., Hettinger, R., Cortina, A.E., Biswas, R.G., Kock, F.V.C., Soong, R., Jenne, A., Du, B., Hou, F., He, H., Lundeen, R., Gilbreath, A., Sutton, R., Scholz, N.L., Davis, J.W., Dodd, M.C., Simpson, A., McIntyre, J.K., Kolodziej, E.P., 2021. A ubiquitous tire rubber–derived chemical induces acute mortality in coho salmon. Science 371, 185–189. https://doi.org/10.1126/science.abd6951.

Totlandsdal, A.I., Johan, Ø., C.R, E., Jan-Inge, H., Kocbach, B.A., Marit, L., Per, S., Edel, L., A, H.J., Kubátová, A., 2014. The occurrence of polycyclic aromatic hydrocarbons and their derivatives and the proinflammatory potential of fractionated extracts of diesel exhaust and wood smoke particles. J. Environ. Sci. Health A Tox. Hazard. Subst. Environ. Eng. https://doi.org/10.1080/10934529.2014.854586.

Upadhyay, R., Khan, H.I.U.-H., Przystaś, W., 2023. An evaluation of decolorization mechanism of synthetic dyes belonging to the azo, anthraquinone, and triphenylmethane group, as a sustainable approach, by immobilized CB8 strain (Trametes versicolor. Desalin. Water Treat. 284, 268–277. https://doi.org/10.5004/dwt.2023.29270.

Vedani, A., Dobler, M., Hu, Z., Smieško, M., 2015. OpenVirtualToxLab—a platform for generating and exchanging in silico toxicity data. Toxicol. Lett. 232, 519–532. https://doi.org/10.1016/j.toxlet.2014.09.004.

Vondráček, J., Švihálková-Šindlerová, L., Pěnčíková, Ki, Marvanová, Sa, Krčmář, P., Ciganek, M., Neča, Jí, Trosko, J.E., Upham, B., Kozubík, A., Machala, M., 2007. Concentrations of methylated naphthalenes, anthracenes, and phenanthrenes occurring in Czech river sediments and their effects on toxic events associated with carcinogenesis in rat liver cell lines. Environ. Toxicol. Chem. 26, 2308–2316. https://doi.org/10.1897/07-161R.1.

Wang, J., Bi, Y., Henkelmann, B., Pfister, G., Zhang, L., Schramm, K.-W., 2016. PAHs and PCBs accumulated by SPMD-based virtual organisms and feral fish in Three Gorges Reservoir, China. Sci. Total Environ. 542, 899–907. https://doi.org/10.1016/j.scitotenv.2015.10.134.

Wang, D.-Q., Yu, Y.-X., Zhang, X.-Y., Zhang, S.-H., Pang, Y.-P., Zhang, X.-L., Yu, Z.-Q., Wu, M.-H., Fu, J.-M., 2012. Polycyclic aromatic hydrocarbons and organochlorine pesticides in fish from Taihu Lake: their levels, sources, and biomagnification. Ecotoxicol. Environ. Safe 82, 63–70. https://doi.org/10.1016/j.ecoenv.2012.05.010.

Wassur, B., 2012. Detoxification mechanisms in fish. University of Gothenburg.

Weiss, V., Gobec, M., Jakopin, Ž., 2024. Halogenation of common phenolic household and personal care product ingredients enhances their AhR-modulating capacity. Chemosphere 350, 141116. Chemosphere 2024, 141116. https://doi.org/10.1016/J.

Whirledge, S., Senbanjo Linda, T., Cidlowski John, A., 2015. Genistein Disrupts Glucocorticoid Receptor Signaling in Human Uterine Endometrial Ishikawa Cells. Environ. Health Persp 123, 80–87. https://doi.org/10.1289/ehp.1408437.

Wilson, C.L., Safe, S., 1998. Mechanisms of ligand-induced aryl hydrocarbon receptor-mediated biochemical and toxic responses. Toxicol. Pathol. 26, 657–671. https://doi.org/10.1177/019262339802600510.

Wolska, L., Mechlińska, A., Rogowska, J., Namieśnik, J., 2012. Sources and fate of PAHs and PCBs in the marine environment. Crit. Rev. Env. Sci. Tec. 42, 1172–1189. https://doi.org/10.1080/10643389.2011.556546.

Won, E.-J., Choi, B., Lee, C.H., Hong, S., Lee, J.-H., Shin, K.-H., 2020. Variability of trophic magnification factors as an effect of estimated trophic position: application of compound-specific nitrogen isotope analysis of amino acids. Environ. Int. 135, 105361. https://doi.org/10.1016/j.envint.2019.105361.

Xiang, T., Shi, C., Guo, Y., Zhang, J., Min, W., Sun, J., Liu, J., Yan, X., Liu, Y., Yao, L., Mao, Y., Yang, X., Shi, J., Yan, B., Qu, G., Jiang, G., 2024. Effect-directed analysis of androgenic compounds from sewage sludges in China. Water Res 256, 121652. https://doi.org/10.1016/j.watres.2024.121652.

Xie, R., Xu, Y., Ma, M., Wang, Z., 2022. An integrated screening strategy for novel AhR agonist candidate identification and toxicity confirmation in sediments. Sci. Total Environ. 842, 156816. https://doi.org/10.1016/j.scitotenv.2022.156816.

Xu, H., George, S.C., Hou, D., 2019. Algal-derived polycyclic aromatic hydrocarbons in Paleogene lacustrine sediments from the Dongying Depression, Bohai Bay Basin, China. Mar. Petrol. Geol. 102, 402–425. https://doi.org/10.1016/j.marpetgeo.2019.01.004.

Yordy, J.E., Wells, R.S., Balmer, B.C., Schwacke, L.H., Rowles, T.K., Kucklick, J.R., 2010. Partitioning of persistent organic pollutants between blubber and blood of wild bottlenose dolphins: implications for biomonitoring and health. Environ. Sci. Technol. 44, 4789–4795. https://doi.org/10.1021/es1004158.

Zhang, Y., Cui, B., Zhang, Q., Liu, X., 2015. Polycyclic aromatic hydrocarbons in the food web of coastal wetlands: distribution, sources and potential toxicity. Clean Soil Air Water 43, 881–891. https://doi.org/10.1002/clen.201400305.

Zhang, W., Xie, H.Q., Li, Y., Zhou, M., Zhou, Z., Wang, R., Hahn, M.E., Zhao, B., 2022. The aryl hydrocarbon receptor: a predominant mediator for the toxicity of emerging dioxin-like compounds. J. Hazard. Mater. 426, 128084. https://doi.org/10.1016/j.jhazmat.2021.128084.

Zhou, Q., Shen, Y., Chou, L., Guo, J., Zhang, X., Shi, W., 2022. Identification of glucocorticoid receptor antagonistic activities and responsible compounds in house dust: bioaccessibility should not be ignored. Environ. Sci. Technol. 56, 16768–16779. https://doi.org/10.1021/acs.est.2c04183.

<Ecotoxicology and Environmental Safety>

Supplementary materials for

Characterization of known and unknown AhR-active substances in freshwater fish from the Gapcheon River, South Korea: Application of effect-directed analysis and nontarget screening

Jihyun Cha, Jiyun Gwak, Junghyun Lee, Dokyun Kim, Eun-Ji Won, Kyung-Hoon Shin, Hyo-Bang Moon, Jong Seong Khim, Seongjin Hong*

This PDF file includes:

Number of pages: 20

Number of Supplementary Tables: 11, Tables S1 to S11

Number of Supplementary Figures: 4, Figures S1 to S4

References

***Corresponding author.** *E-mail address*: hongseongjin@cnu.ac.kr (S. Hong).

Supplementary Tables

Table S1. Biological information of fish samples collected from the Gapcheon River, Daejeon, South Korea.

Common name (Sample id & scientific name)	Body length (cm)	Body weight (g)	Stable isotope ratios (‰)			Trophic positions		Target organ	Lipid contents (%)
			$\delta^{13}C_{bulk}$	$\delta^{15}N_{bulk}$	$\delta^{15}N_{Glu\text{-}Phe}$	TP_{bulk}	TP_{AAs}		
Crucian carp (S1) (*Carassius carassius*)	30	350	–23.9	9.1	11.9	2.5	2.2	Bladder	2.0
								Muscle	4.0
								Egg	7.0
Common carp (S2) (*Cyprinus carpio*)	57	1920	–23.8	11.8	11.5	3.3	2.2	Liver	6.6
Far Eastern catfish (S3) (*Silurus asotus*)	45	440	–23.4	12.4	17.1	3.4	3.0	Muscle	5.5
								Fillet	2.0
Barbel steed (S4) (*Hemibarbus labeo*)	60	1740	–23.5	13.8	18.7	3.9	3.2	Liver	3.6
Skygager (S5) (*Erythroculter erythropterus*)	62	1190	–23.1	13.5	18.4	3.8	3.2	Liver	2.5

Table S2. List of target compounds, abbreviations, log K_{OW} values, quantification and confirmation ions, and method detection limits in the analysis of polychlorinated biphenyls (PCBs), traditional polycyclic aromatic hydrocarbons (t-PAHs), and emerging PAHs (e-PAHs).

Compounds	Abb.[a]	Log K_{OW}[b]	Quantification ion	Confirmation ion	LOD[c] (ng g^{-1} dm)
Polychlorinated biphenyls (PCBs)					
2,4'-Dichlorobiphenyl	CB 8	5.09	222	224	0.01
2,4,4'-Trichlorobiphenyl	CB 28	5.62	256	258	0.03
2,2',5,5'-Tetrachlorobiphenyl	CB 52	5.84	292	290	0.02
2,2',4,5'-Tetrachlorobiphenyl	CB 49	5.85	292	290	0.02
2,2',3,5'-Tetrachlorobiphenyl	CB 44	5.75	292	290	0.03
3,4,4'-Trichlorobiphenyl	CB 37	5.83	256	258	0.02
2,4,4',5-Tetrachlorobiphenyl	CB 74	6.20	292	290	0.02
2,3',4',5-Tetrachlorobiphenyl	CB 70	6.20	292	290	0.01
2,3',4,4'-Tetrachlorobiphenyl	CB 66	6.20	292	290	0.03
2,3,4,4'-Tetrachlorobiphenyl	CB 60	6.11	292	290	0.03
2,2',4,5,5'-Pentachlorobiphenyl	CB 101	6.38	326	324	0.02
2,2',4,4',5-Pentachlorobiphenyl	CB 99	6.39	326	328	0.02
2,2',3,4,5'-Pentachlorobiphenyl	CB 87	6.29	292	290	0.02
3,3',4,4'-Tetrachlorobiphenyl	CB 77	6.36	326	256	0.01
2,2',3,3',4-Pentachlorobiphenyl	CB 82	6.20	338	340	0.03
2,3',4,4',5-Pentachlorobiphenyl	CB 118	6.74	326	328	0.03
2,3,4,4',5-Pentachlorobiphenyl	CB 114	6.30	326	328	0.02
2,2',4,4',5,5'-Hexachlorobiphenyl	CB 153	6.83	360	362	0.02
2,3,3',4,4'-Pentachlorobiphenyl	CB 105	6.65	326	324	0.02
2,2',3,3',5,6,6'-Heptachlorobiphenyl	CB 179	7.03	396	398	0.03
2,2',3,4,4',5'-Hexachlorobiphenyl	CB 138	6.83	360	362	0.02
2,3,3',4,4',6-Hexachlorobiphenyl	CB 158	6.79	326	328	0.03
3,3',4,4',5-Pentachlorobiphenyl	CB 126	6.45	360	362	0.02
2,3,4,4',5,6-Hexachlorobiphenyl	CB 166	6.61	394	396	0.02
2,2',3,4',5,5',6-Heptachlorobiphenyl	CB 187	7.17	394	396	0.02
2,2',3,4,4',5',6-Heptachlorobiphenyl	CB 183	7.20	360	362	0.02
2,2',3,3',4,4'-Hexachlorobiphenyl	CB 128	6.74	440	442	0.02
2,3,3',4,4',5-Hexachlorobiphenyl	CB 156	7.18	360	362	0.02
2,2',3,4,4',5,5'-Heptachlorobiphenyl	CB 180	7.17	394	396	0.03
3,3',4,4',5,5'-Hexachlorobiphenyl	CB 169	7.16	360	362	0.03
2,2',3,3',4,4',5-Heptachlorobiphenyl	CB 170	7.27	394	396	0.03
2,3,3',4,4',5,5'-Heptachlorobiphenyl	CB 189	7.20	476	478	0.03
Traditional polycyclic aromatic hydrocarbons (t-PAHs)					
Acenaphthylene	Acl	3.94	152	151	0.06
Acenaphthene	Ace	3.92	153	154	0.12
Fluorene	Flu	4.18	166	165	0.15
Phenanthrene	Phe	4.46	178	176	0.06
Anthracene	Ant	4.45	178	176	0.07
Fluoranthene	Fl	5.16	202	200	0.09
Pyrene	Py	4.88	202	200	0.12
Benzo[*a*]anthracene	BaA	5.76	228	226	0.06
Chrysene	Chr	5.81	228	226	0.03
Benzo[*b*]fluoranthene	BbF	5.78	252	253	0.08
Benzo[*k*]fluoranthene	BkF	6.11	252	253	0.10
Benzo[*a*]pyrene	BaP	5.99	252	253	0.08
Indeno[*1,2,3-cd*]pyrene	IcdP	6.76	276	138	0.09
Benzo[*g,h,i*]perylene	BghiP	6.70	276	138	0.12
Dibenz[*a,h*]anthracene	DbahA	6.54	278	276	0.07

Emerging PAHs (e-PAHs)					
11H-Benzo[*a*]fluorene	11BaF	5.10	216	215	0.04
11H-Benzo[*b*]fluorene	11BbF	5.77	216	215	0.04
Benzo[*b*]naphtho[*2,3-d*]furan	BBNF	5.05	218	189	0.32
Benzo[*b*]anthracene	BbA	5.76	228	226	0.12
Benzo[*b*]naphtho[*2,1-d*]thiophene	BBNT	5.19	234	235	0.11
4,5-Methanochrysene	4,5MC	5.78	239	240	0.04
5-Methylbenzo[*a*]anthracene	5MbA	6.07	242	241	0.20
1-Methylchrysene	1MC	6.07	242	241	0.14
3-Methylchrysene	3MC	6.07	242	239	0.12
7-Methylbenz[*a*]anthracene	7MbA	6.07	242	241	0.09
Benzo[*j*]fluoranthene	BjF	5.78	252	253	0.52
7,12-Dimethylbenz[*a*]anthracene	7,12DbA	5.80	256	241	0.05
10-Methylbenzo[*a*]pyrene	10MbA	6.66	266	256	0.01
20-Methylcholanthrene	20Mc	6.42	268	252	0.02
Internal standard					
2-Fluorobiphenyl	IS		172	171	

[a] Abb.: Abbreviation.
[b] The log K_{OW} values of the chemicals were obtained from ChemSpider (www.chemspider.com).
[c] LOD.: Limit of detection.

Table S3. Instrumental conditions for the analysis of PCBs in fish extracts using GC-MS/MS.

Instrument	GC: Agilent Technologies 7890B, MS/MS: Agilent Technologies 7000C
Samples	F1 from fish extracts
Analytical column	HP-5MS (30 m × 0.25 mm i.d. × 0.25 μm film)
Carrier gas	Helium
Injection volume	1.0 μL
Flow rate	1.0 mL min^{-1}
Mass range	50–600 *m/z*
Ion source temperature	230 ℃
Ionization mode	EI mode (70 eV)
Oven temperature	75 ℃ (hold 2 min) → 15 ℃ min^{-1} to 150 ℃ (hold 0 min) → 2.5 ℃ min^{-1} to 250 ℃ (hold 5 min)

Table S4. Instrumental conditions for the analysis of t-PAHs and e-PAHs in fish extracts using GC-MSD.

Instrument	GC: Agilent Technologies 7890B, MSD: Agilent Technologies 5977B
Samples	F2 from fish extracts
Analytical column	DB-5MS (30 m × 0.25 mm i.d. × 0.25 μm film)
Carrier gas	Helium
Injection volume	1.0 μL
Flow rate	1.0 mL min^{-1}
Mass range	50–600 *m/z*
Ion source temperature	230 °C
Ionization mode	EI mode (70 eV)
Oven temperature	60 °C (hold 2 min) → 6 °C min^{-1} to 300 °C (hold 13 min)

Table S5. Relative potency values of known AhR agonists (t-PAHs and e-PAHs) compared to benzo[a]pyrene, as reported in previous studies.

Compounds	Effective concentrations[a]	Relative potency values	References
t-PAHs			
BaA	EC_{50}	3.2×10^{-1}	Kim et al. (2019)
Chr	EC_{50}	8.5×10^{-1}	
BbF	EC_{50}	5.0×10^{-1}	
BkF	EC_{50}	4.8×10^{-1}	
BaP	EC_{50}	1.0	
IcdP	EC_{50}	5.8×10^{-1}	
DbahA	EC_{50}	6.6×10^{-1}	
e-PAHs			
11BaF	EC_{50}	1.2	Cha et al. (2019)
4,5MC	EC_{50}	1.0	
BbA	EC_{50}	10.6	
10MbA	EC_{50}	1.2	Gwak et al. (2022)
20Mc	EC_{50}	3.2	
7MbA	EC_{50}	1.4	
7,12DbA	EC_{50}	2.0×10^{-1}	
11BbF	EC_{50}	2.4×10^{-1}	Kim et al. (2019)
BBNT	EC_{50}	3.6×10^{-2}	
BBNF	EC_{50}	8.2×10^{-2}	
BjF	EC_{50}	1.7	
5MbA	EC_{50}	4.2×10^{-1}	
1MC	EC_{50}	6.0	
3MC	EC_{50}	1.5	

[a]: Relative potency values for AhR agonists were calculated based on the effective concentration at the 50% level observed for benzo[*a*]pyrene.

Table S6. Instrumental conditions for GC-QTOFMS used in the nontarget screening of F2 from S1 muscle, S1 egg, S3 fillet, and S5 liver extracts collected from Gapcheon River, South Korea.

Instrument	GC: Agilent Technologies 7890B; QTOFMS: Agilent Technologies 7200
Samples	F2 from S1 muscle, S1 egg, S3 fillet, and S5 liver extracts
Inlet temperature	240 °C
Column	DB-5MS UI (30 m × 0.25 mm i.d. × 0.25 μm film)
Oven temperature	50 ℃ (3 min) – 150 ℃ (10℃/min) – 240 ℃ (20 ℃/min, 10 min)
Carrier gas	Helium
Flow rate	1.2 mL $min.^{-1}$
Injection volume	2 μL
Transfer line temperature	250 ℃
Ionization mode	EI mode (70 eV)
Ion source temperature	230 °C
Mass range	50–1000 *m*/*z*
Scan speed	3 spectra/sec
Monitoring mode	4 Ghz high-resolution
Software	Qualitative analysis B.07.01 MassHunter Quantitative analysis Unknown analysis NIST Library (ver. 2017)

Table S7. Concentrations of Hg, PCBs, t-PAHs, and e-PAHs in fish samples collected from the Gapcheon River, South Korea.

Compounds	S1 Bladder	S1 Muscle	S1 Egg	S2 Liver	S3 Muscle	S3 Fillet	S4 Liver	S5 Liver
Hg (ng g^{-1} dm)								
Hg	36	180	17	500	420	620	900	1100
PCBs (ng g^{-1} lm)								
CB 8	ND[a]	ND	ND	ND	37	78	43	63
CB 28	ND	40	ND	24	ND	ND	ND	63
CB 52	54	30	15	ND	ND	ND	ND	ND
CB 49	ND	46	ND	28	ND	ND	ND	ND
CB 44	ND	51	ND	30	ND	ND	63	ND
CB 37	91	45	ND	27	44	90	ND	ND
CB 74	ND	44	ND	ND	ND	ND	ND	70
CB 70	ND	ND	ND	ND	ND	ND	50	ND
CB 66	76	38	ND	23	36	ND	44	ND
CB 60	ND	ND	ND	ND	ND	ND	ND	ND
CB 101	ND	33	18	19	ND	ND	ND	56
CB 99	ND	ND	ND	23	ND	ND	ND	70
CB 87	ND	ND	ND	ND	ND	ND	21	68
CB 77	ND	ND	ND	ND	ND	ND	ND	ND
CB 82	ND	ND	ND	ND	ND	ND	ND	64
CB 118	ND	ND	ND	ND	29	ND	ND	50
CB 114	ND	28	ND	ND	27	ND	39	48
CB 153	ND	53	26	34	ND	ND	66	ND
CB 105	ND	35	19	ND	32	68	39	57
CB 179	54	29	13	16	42	ND	71	49
CB 138	ND	ND	ND	ND	ND	ND	ND	ND
CB 158	ND	ND	ND	ND	50	ND	ND	ND
CB 126	ND	ND	ND	42	ND	ND	78	117
CB 166	ND	ND	ND	13	ND	ND	ND	ND
CB 187	ND	44	27	27	ND	ND	61	ND
CB 183	ND	48	27	ND	ND	ND	54	ND
CB 128	ND	ND	ND	ND	ND	ND	ND	ND
CB 156	ND	ND	ND	25	ND	ND	ND	ND
CB 180	ND	ND	34	ND	ND	ND	71	ND
CB 169	ND	ND	ND	ND	ND	ND	ND	ND
CB 170	ND	37	21	ND	ND	ND	ND	58
CB 189	ND	ND	ND	ND	ND	ND	ND	118
SUM	280	600	200	330	300	240	700	950
t-PAHs (ng g^{-1} lm)								
Acl	54	22	14	28	30	85	38	44
Ace	310	90	66	110	160	310	200	250
Flu	2200	640	480	620	1100	2000	940	1400
Phe	3800	1400	700	1000	1500	2800	1800	2400
Ant	ND	ND	ND	ND	ND	ND	ND	ND
Fl	320	270	120	120	150	330	260	250
Py	ND	ND	ND	ND	ND	ND	ND	ND
BaA	ND	ND	ND	ND	ND	150	ND	ND
Chr	120	77	37	43	57	180	58	66
BbF	ND	ND	ND	ND	ND	ND	ND	ND
BkF	ND	79	64	16	11	68	ND	ND
BaP	21	30	10	24	65	71	37	41
IcdP	ND	ND	ND	ND	ND	ND	ND	ND
BghiP	ND	ND	28	ND	ND	ND	ND	ND

DbahA	100	ND	ND	ND	ND	ND	10	13
SUM	6900	2600	1500	2000	3000	6000	3300	4500
e-PAHs (ng g^{-1} lm)								
11BaF	ND	17	ND	ND	ND	ND	16	ND
11BbF	23	7.0	ND	7.8	12	45	24	12
BBNF	80	200	84	70	48	140	210	130
BbA	130	21	63	60	120	220	140	190
BBNT	ND	ND	ND	ND	ND	29	ND	ND
4,5MC	16	6.9	3.7	4.3	6.1	18	7.7	11
5MbA	ND	ND	ND	ND	ND	ND	ND	ND
1MC	ND	ND	ND	ND	ND	ND	ND	ND
3MC	63	29	21	13	28	98	45	42
7MbA	ND	ND	ND	ND	ND	ND	ND	ND
BjF	ND	ND	ND	ND	ND	ND	ND	ND
7,12DbA	ND	ND	8.7	5.2	ND	ND	ND	ND
10MbA	4.4	ND	1.6	1.0	1.0	ND	ND	5.8
20Mc	4.6	5.2	3.4	1.8	3.7	17	9.4	19
SUM	320	290	190	160	220	560	450	420

[a] ND: Not detected.

Table S8. Number of AhR agonist candidates detected in F2 from S1 muscle, S1 egg, S3 fillet, and S5 liver extracts at each step of the six-step selection process.

Samples	Step 1	Step 2	Step 3	Step 4	Step 5	Step 6
S1 Muscle	1911	516	226	145	76	12
S1 Egg	1950	563	251	167	81	7
S3 Fillet	1792	488	185	108	53	2
S5 Liver	3003	902	355	247	95	3

Table S9. List of AhR agonist candidates detected in F2 from S1 muscle, S1 egg, S3 fillet, and S5 liver extracts using GC-QTOFMS.

Sample and compounds	Molecular formula	CAS number	Molar mass	Matching factor	Peak intensity	Log Kow[a]	Uses	References
S1 Muscle								
Triphenylmethane	$C_{19}H_{16}$	519-73-3	244.337	95	3.5×10^6	5.4	Dye precursors	Upadhyat et al. (2013)
2-Methylanthracene	$C_{15}H_{12}$	613-12-7	192.261	94	3.4×10^5	5.1	Combustion byproducts	An et al. (2020)
1-Methylphenanthrene	$C_{15}H_{12}$	832-69-9	192.261	88	2.5×10^5	5.1	Crude oil & vehicle emissions	Huang et al. (2017)
2-Methyltriphenylene	$C_{19}H_{14}$	1705-84-6	242.321	84	1.0×10^5	6.4	Combustion byproducts	Xu et al. (2017)
o-Terphenyl	$C_{18}H_{14}$	84-15-1	230.310	83	1.7×10^5	5.5	Industrial materials	Mansi et al. (2021)
2-Isopropyl-10-methylphenanthrene	$C_{18}H_{18}$	66552-97-4	234.342	83	1.8×10^5	6.4	Crude oil & vehicle emissions	Ndabambi et al. (2021)
10,18-Bisnorabieta-8,11,13-triene	$C_{18}H_{26}$	32624-67-2	242.406	78	3.9×10^6	7.3	Combustion byproducts	Sapozhnikova and Hoh (2019)
4-Methylpyrene	$C_{17}H_{12}$	3353-12-6	216.283	78	4.6×10^4	5.6	Crude oil & vehicle emissions	Ogbesejana et al. (2019)
Dehydroabietine	$C_{19}H_{28}$	5323-56-8	256.433	76	1.4×10^6	7.8	Combustion byproducts	Prokes and Hlozek (2007)
1,1,3,3-Tetraphenyl-1,3-dimethyldisiloxane	$C_{26}H_{26}OSi_2$	807-28-3	410.665	72	1.6×10^5	9.9	Silicone-based compounds	Itoh and Yang (2002)
9-Methylanthracene	$C_{15}H_{12}$	779-02-2	192.261	72	2.0×10^5	5.1	Combustion byproducts	Bae et al. (2018)
Abietatriene	$C_{20}H_{30}$	19407-28-4	270.460	72	3.8×10^5	8.3	Natural product	Fan et al. (2017)
S1 Egg								
Triphenylmethane	$C_{19}H_{16}$	519-73-3	244.337	90	3.2×10^6	5.4	Dye precursors	Upadhyat et al. (2013)
3-Methylphenanthrene	$C_{15}H_{12}$	832-71-3	192.261	89	2.6×10^5	4.9	Crude oil & vehicle emissions	Ndabambi et al. (2021)
4-Cyclohexylbiphenyl	$C_{18}H_{20}$	3842-58-8	236.358	85	4.6×10^5	6.6	Unknown	
7-Isopropyl-1-methyl-1,2,3,4-tetrahydrophenanthrene	$C_{18}H_{22}$	6566-19-4	238.374	81	2.6×10^5	7.0	Crude oil & vehicle emissions	Ndabambi et al. (2021)
1-Methyltriphenylene	$C_{19}H_{14}$	2871-91-2	242.321	80	7.7×10^4	6.1	Combustion byproducts	Xu et al. (2019)
o-Terphenyl	$C_{18}H_{14}$	84-15-1	230.310	78	1.1×10^5	5.5	Industrial materials	Mansi et al. (2021)

2,4,5,7-Tetramethylphenanthrene	$C_{17}H_{18}$	7396-38-5	234.342	73	8.8×10^4	6.5	Crude oil & vehicle emissions	Ndabambi et al. (2021)
S3 Fillet								
Triphenylmethane	$C_{19}H_{16}$	519-73-3	244.337	96	3.6×10^6	5.4	Dye precursors	Upadhyat et al. (2013)
Phthalic acid, 3,5-dimethylphenyl 3-methylphenyl ester	$C_{23}H_{20}O_4$	997745-35-9	360.409	71	9.1×10^4	5.8	Unknown	
S5 Liver								
Triphenylmethane	$C_{19}H_{16}$	519-73-3	244.337	96	3.6×10^6	5.4	Dye precursors	Upadhyat et al. (2013)
2-Isopropyl-10-methylphenanthrene	$C_{18}H_{18}$	66552-97-4	234.342	82	3.2×10^5	6.4	Crude oil & vehicle emissions	Ndabambi et al. (2021)
9-Propylphenanthrene	$C_{17}H_{16}$	17024-03-2	220.315	76	9.3×10^4	5.9	Crude oil & vehicle emissions	Ndabambi et al. (2021)

[a] Log K_{ow} values were obtained from ChemSpider.

Table S10. Predicted potential toxic effects of AhR agonist candidates in F2 from S1 muscle, S1 egg, S3 fillet, and S5 liver extracts, assessed using VirtualToxLab in silico modeling.

Samples and compounds	PubChem CID	AhR	AR	ER	GR	TR
S1 Muscle						
Triphenylmethane	10614	0.523[a]	0.235	0.318	0.301	0.324
2-Methylanthracene	11936	0.333	0.107	0.164	0.161	0.171
1-Methylphenanthrene	13257	0.315	0.095	0.152	0.145	0.153
2-Methyltriphenylene	618051	0.372	0.137	0.193	0.195	0.208
o-Terphenyl	6766	0.476	0.198	0.280	0.264	0.281
2-Isopropyl-10-methylphenanthrene	613068	0.410	0.154	0.216	0.223	0.223
10,18-Bisnorabieta-8,11,13-triene	614842	0.439	0.158	0.236	0.232	0.224
4-Methylpyrene	18784	0.311	0.094	0.163	0.158	0.167
Dehydroabietine	220273	0.427	0.169	0.227	0.239	0.222
1,1,3,3-Tetraphenyl-1,3-dimethyldisiloxane	13121	0.426	0.232	0.372	0.311	0.310
9-Methylanthracene	13068	0.330	0.104	0.162	0.163	0.167
Abietatriene	86869	0.373	0.158	0.218	0.226	0.222
S1 Egg						
Triphenylmethane	10614	0.523	0.235	0.318	0.301	0.324
3-Methylphenanthrene	13258	0.313	0.096	0.155	0.153	0.161
4-Cyclohexylbiphenyl	119782	0.489	0.212	0.290	0.278	0.286
7-Isopropyl-1-methyl-1,2,3,4-tetrahydrophenanthrene	613986	0.431	0.168	0.236	0.239	0.233
1-Methyltriphenylene	76131	0.388	0.128	0.193	0.192	0.200
o-Terphenyl	6766	0.476	0.198	0.280	0.264	0.281
2,4,5,7-Tetramethylphenanthrene	23880	0.340	0.111	0.165	0.162	0.176
S3 Fillet						
Triphenylmethane	10614	0.523	0.235	0.318	0.301	0.324
Phthalic acid, 3,5-dimethylphenyl 3-methylphenyl ester	6425688	0.334	0.285	0.258	0.365	0.211
S5 Liver						
Triphenylmethane	10614	0.523[a]	0.235	0.318	0.301	0.324
2-Isopropyl-10-methylphenanthrene	613068	0.410	0.154	0.216	0.223	0.223
9-Propylphenanthrene	100647	0.384	0.136	0.205	0.202	0.221

[a] 0.0−0.2: no binding, 0.2−0.4: low binding, 0.4−0.6: moderate binding, 0.6−0.8: high binding.

Table S11. Predicted additional toxic effects of AhR agonist candidates in F2 from S1 muscle, S1 egg, S3 fillet, and S5 liver extracts using VEGA QSAR models.

Compounds	Carcinogenicity[a]	Developmental toxicity[b]	Mutagenicity[c]
S1 Muscle			
Triphenylmethane	–[d] +[e] – –	+ +	– – – – –
2-Methylanthracene	+ + – +	– +	+ + + + +
1-Methylphenanthrene	+ + + +	– +	+ + + + +
2-Methyltriphenylene	+ + – +	– –	+ + + + +
o-Terphenyl	– + – –	– +	– – – – –
2-Isopropyl-10-methylphenanthrene	+ + + +	– +	+ + + + +
10,18-Bisnorabieta-8,11,13-triene	– + + –	– +	– – – – –
4-Methylpyrene	+ + + –	– +	+ + + + +
Dehydroabietine	– + + –	– +	– – – – –
1,1,3,3-Tetraphenyl-1,3-dimethyldisiloxane	– – – –	+ +	– – – – –
9-Methylanthracene	+ + + +	– +	+ + + + +
Abietatriene	– + + –	– +	– – – – –
S1 Egg			
Triphenylmethane	– + – –	+ +	– – – – –
3-Methylphenanthrene	+ + – +	– +	+ + + + +
4-Cyclohexylbiphenyl	– + – –	– +	– + – – –
7-Isopropyl-1-methyl-1,2,3,4-tetrahydrophenanthrene	– + + +	– +	+ + – + –
1-Methyltriphenylene	+ + + +	– +	+ + + + +
o-Terphenyl	– + – –	– +	– – – – –
2,4,5,7-Tetramethylphenanthrene	+ + + +	– +	– – – – –
S3 Fillet			
Triphenylmethane	– + – –	+ +	– – – – –
Phthalic acid, 3,5-dimethylphenyl 3-methylphenyl ester	+ – – –	– –	– – – – –
S5 Liver			
Triphenylmethane	– + – –	+ +	– – – – –
2-Isopropyl-10-methylphenanthrene	+ + + +	– +	+ + + + +
9-Propylphenanthrene	+ + + +	– +	+ – + + +

[a] Carcinogenic potential of AhR agonist candidates predicted using VEGA QSAR with four models (ISS, CAESAR, IRFMN/Antares, and IRFMN/ISSCAN-CGX).

[b] Developmental toxicity of AhR agonist candidates predicted using VEGA QSAR with two models (PG and CAESAR).

[c] Mutagenicity potential of AhR agonist candidates predicted using VEGA QSAR with five models (SarPy/IRFMN, KNN/Read-Across, ISS, CONSENSUS, and CAESAR)

[d] –: Not active.

[e] +: Active.

Supplementary Figures

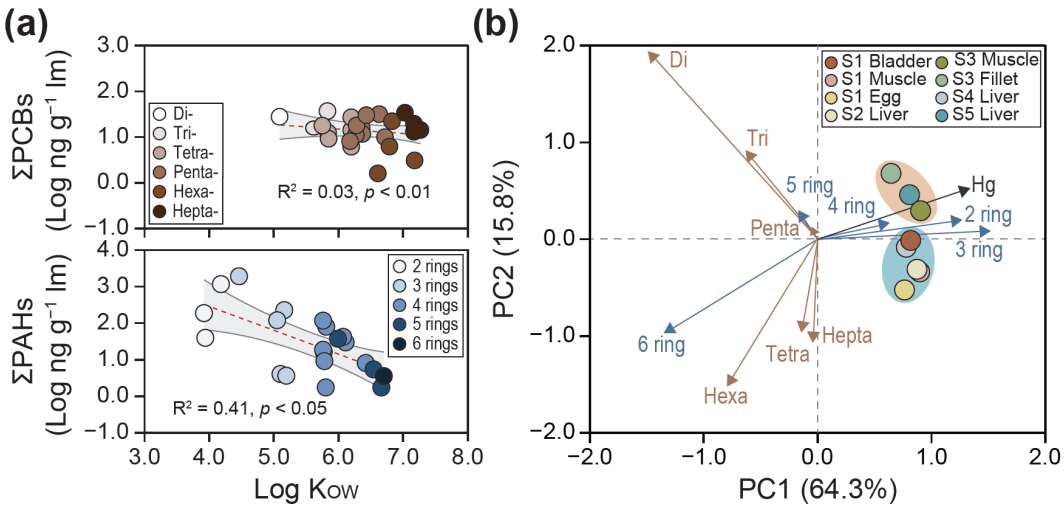

Fig. S1. (a) Relationship between PCB and PAH concentrations and log K_{OW} values in fish extracts. The shaded area represents the 95% confidence interval. **(b)** PCA results based on the concentrations and compositions of Hg, PCBs, and PAHs in fish collected from Gapcheon River, South Korea.

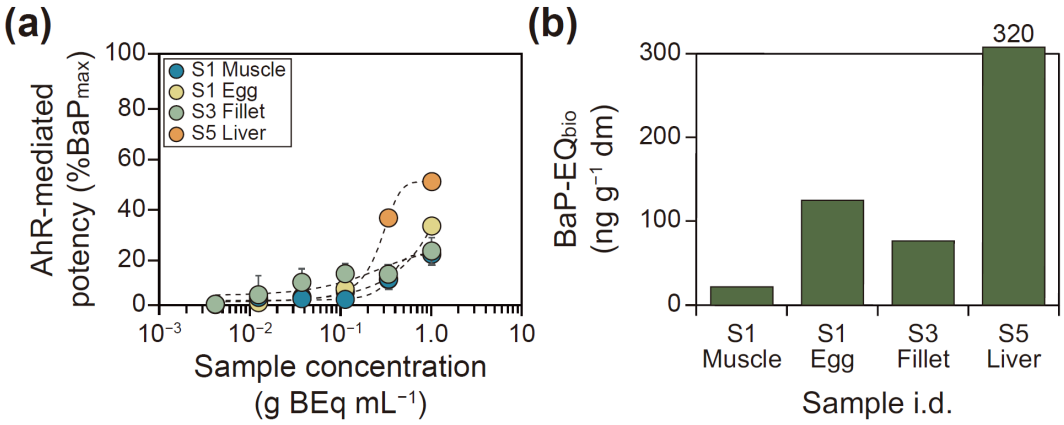

Fig. S2. (a) Dose-response curves for F2 of fish extracts with BaP_{max} values exceeding 20% after 4-hour exposure in the H4IIE-*luc* bioassay. Error bars represent the mean ± standard deviation (n = 3). **(b)** BaP-EQ_{bio} concentrations in F2 from S1 muscle, S1 egg, S3 fillet, and S5 liver extracts, where BaP_{max} values exceeded 20%. These concentrations were used for potency balance analysis.

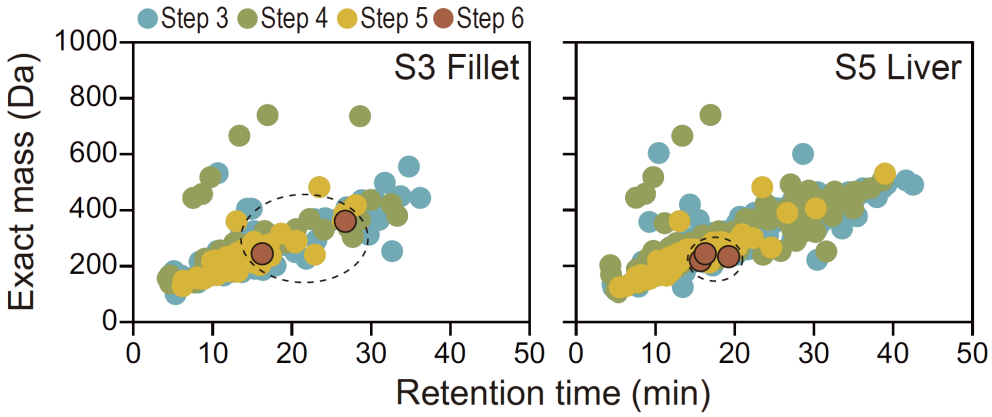

Fig. S3. Retention time and exact mass distribution of AhR agonist candidates refined through the selection process in F2 from S3 fillet and S5 liver samples.

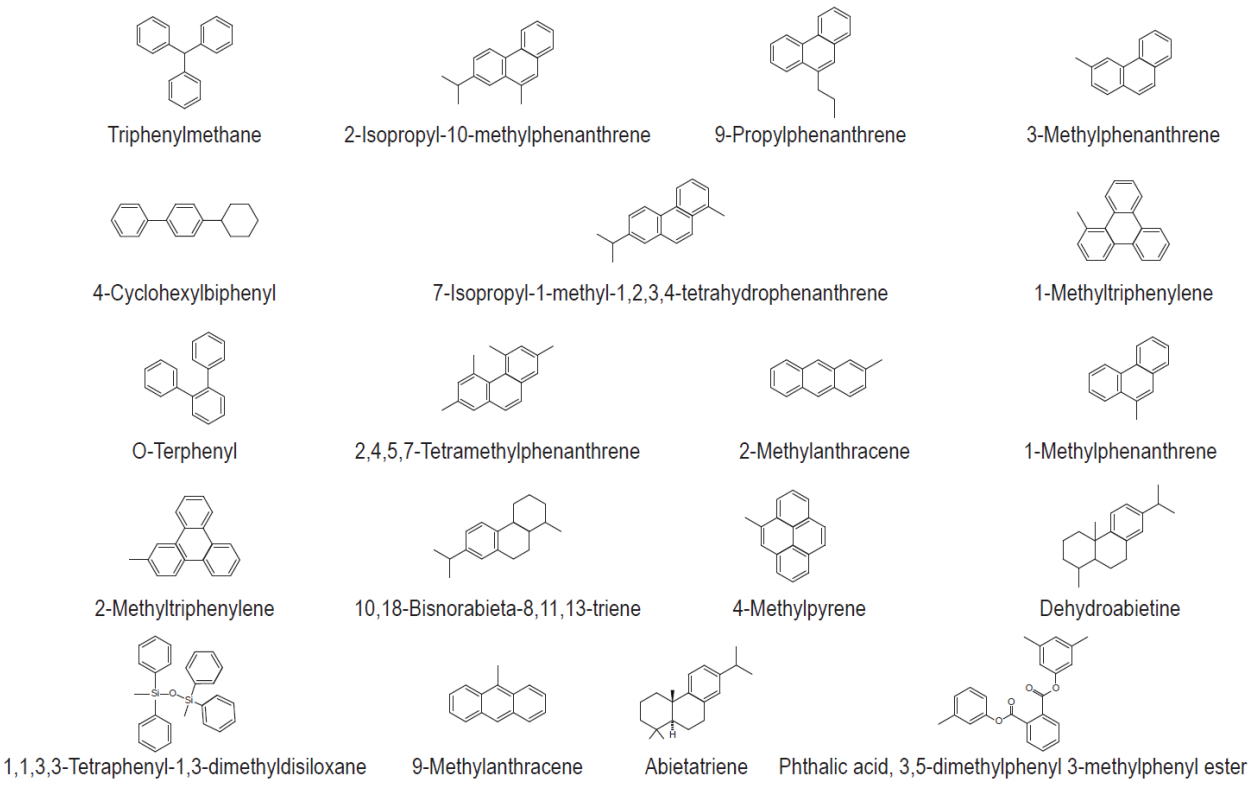

Fig. S4. Chemical structures of the 19 AhR agonist candidates identified in F2 from S1 muscle, S1 egg, S3 fillet, and S5 liver extracts collected from the Gapcheon River, South Korea.

References

An, Y., Hong, S., Kim, Y., Kim, M., Choi, B., Won, E.-J., Shin, K.-H., 2020. Trophic transfer of persistent toxic substances through a coastal food web in Ulsan Bay, South Korea: Application of compound-specific isotope analysis of nitrogen in amino acids. Environ. Pollut. 266, 115160. https://doi.org/10.1016/j.envpol.2020.115160.

Bae, M.-S., Park, J.K., Kim, K.-H., Cho, S.-S., Lee, K.-Y. and Shon, Z.-H., 2018. Emission and Cytotoxicity of Surgical Smoke: Cholesta-3,5-Diene Released from Pyrolysis of Prostate Tissue. Atmosphere 9, 381. https://doi.org/10.3390/atmos9100381.

Cha, J., Hong, S., Kim, J., Lee, J., Yoon, S.J., Lee, S., Moon, H.B., Shin, K.H., Hur, J., Giesy, J.P., Khim, J.S., 2019. Major AhR-active chemicals in sediments of Lake Sihwa, South Korea: application of effect-directed analysis combined with full-scan screening analysis. Environ. Int. 133, 105199. https://doi.org/10.1016/j.envint.2019.105199.

Fan, D., Zhou, S., Zheng, Z., Zhu, G.-Y., Yao, X., Yang, M.-R., Jiang, Z.-H., Bai, L.-P., 2017. New Abietane and Kaurane Type Diterpenoids from the Stems of *Tripterygium regelii*. Int. J. Mol. Sci. 18, 147. https://doi.org/10.3390/ijms18010147.

Gwak, J., Cha, J., Lee, J., Kim,Y., An, S.A., Lee, S., Moon, H.-B., Hur, J., Giesy, J.P, Hong, S., Khim, J.S., 2022. Effect-directed identification of novel aryl hydrocarbon receptor-active aromatic compounds in coastal sediments collected from a highly industrialized area. Sci. Total Environ. 803,149969. https://doi.org/10.1016/j.scitotenv.2021.149.

Itoh, T. and Yang, M.-H., 2002. Temperature dependence of the fluorescence quantum yields of diphenylsiloxane-based copolymers in dilute solutions. J. Polym. Sci. Pol. Phys. 40, 854–861. https://doi.org/10.1002/polb.10151.

Kim, J., Hong, S., Cha, J., Lee, J., Kim, T., Lee, S., Moon, H.B., Shin, K.H., Hur, J., Lee, J.S., Giesy, J.P., Khim, J.S., 2019. Newly identified AhR-active compounds in the sediments of an industrial area using effect-directed analysis. Environ. Sci. Technol. 53, 10043–10052. https://doi.org/10.1021/acs.est.9b02166.

Ndabambi, M., Kim, K.Y., Jung, J.-H., Yim, U.-H., Oh, J.-E., 2021. Alkylated phenanthrene distributions in black rockfish (*Sebastes schlegelii*) and biotransformation into hydroxylated metabolites after intragastric administration. Sci. Total Environ. 762, 143160. https://doi.org/10.1016/j.scitotenv.2020.143160.

Ogbesejana, A.B., Sonibare, O.O. and Ningning, Z., 2019. Occurrence and distribution of pyrene and its derivatives in crude oils and source rock extracts from Niger Delta, Nigeria. J. Pet. Technol. 9, 3–17.

Prokes, L. and Hlozek, M., 2007. Identification of some adhesives and wood pyrolysis products of archaeological origin by direct inlet mass spectrometry. Chem. Anal 52, 700–713.

Sapozhnikova, Y. and Hoh, E., 2019. Suspect screening of chemicals in food packaging plastic film by comprehensive two-dimensional gas chromatography coupled to time-of-flight mass spectrometry. LC GC N. Am. 37, 52–65.

Upadhyay, R., Khan, H.I.U.-H., Przystaś, W., 2023. An evaluation of decolorization mechanism of synthetic dyes belonging to the azo, anthraquinone, and triphenylmethane group, as a sustainable approach, by immobilized CB8 strain (Trametes versicolor). Desalin. Water Treat. 284, 268–277. https://doi.org/10.5004/dwt.2023.29270.

Xu, H., George, S.C., Hou, D., 2019. Algal-derived polycyclic aromatic hydrocarbons in Paleogene lacustrine sediments from the Dongying Depression, Bohai Bay Basin, China. Mar. Petrol. Geol. 102, 402–425. https://doi.org/10.1016/j.marpetgeo.2019.01.004.